NCEP NOTES

Performance of NCEP Regional Wave Models in Predicting Peak Sea States during the 2005 North Atlantic Hurricane Season*

YUNG Y. CHAO AND HENDRIK L. TOLMAN

NOAA/NCEP/Environmental Modeling Center/Marine Modeling and Analysis Branch, Camp Springs, Maryland

(Manuscript received 4 June 2009, in final form 16 April 2010)

ABSTRACT

Unprecedented numbers of tropical cyclones occurred in the North Atlantic Ocean and the Gulf of Mexico in 2005. This provides a unique opportunity to evaluate the performance of two operational regional wave forecasting models at the National Centers for Environmental Prediction (NCEP). This study validates model predictions of the tropical cyclone–generated maximum significant wave height, simultaneous spectral peak wave period, and the time of occurrence against available buoy measurements from the National Data Buoy Center (NDBC). The models used are third-generation operational wave models: the Western North Atlantic wave model (WNA) and the North Atlantic Hurricane wave model (NAH). These two models have identical model physics, spatial resolutions, and domains, with the latter model using specialized hurricane wind forcing. Both models provided consistent estimates of the maximum wave height and period, with random errors of typically less than 25%, and timing errors of typically less than 5 h. Compared to these random errors, systematic model biases are negligible, with a typical negative model bias of 5%. It appears that higher wave model resolutions are needed to fully utilize the specialized hurricane wind forcing, and it is shown that present routine wave observations are inadequate to accurately validate hurricane wave models.

1. Introduction

The Atlantic hurricane season of 2005 was extraordinary not only for its early beginning and late ending (May–December) but also for the number and the intensity of tropical cyclones. According to the National Climatic Data Center (NCDC 2006), there was a record of 27 named tropical cyclones, of which 15 were hurricanes. Among these storms, seven were major hurricanes of category 3 or higher (i.e., hurricanes Dennis, Emily, Katrina, Maria, Rita, Wilma, and Beta). Four of them reached category 5 (Emily, Katrina, Rita, and Wilma), in which Hurricane Katrina was the most intense and destructive land-falling hurricane on record for the Atlantic basin. Many of these tropical cyclones have created high waves disastrous to the coastal areas and offshore marine activities (in particular, oil exploration and production). Extensive measurements of wind and wave conditions made by the National Data Buoy Center (NDBC) provide an excellent opportunity to validate the National Centers for Environmental Prediction (NCEP) operational regional wave models.

There are two operational regional wave models that forecast sea states over the western North Atlantic Ocean domain at NCEP. These are the Western North Atlantic wave model (WNA) and the North Atlantic Hurricane wave model (NAH) (Chao et al. 2003a,b, 2005). They are part of the National Oceanic and Atmosphere Administration's global wave forecasting suite, NOAA WAVEWATCH III (NWW3; Tolman 2002a; Tolman et al. 2002). The performance of the forecast guidance produced by the WNA and NAH models for sea states generated by Hurricane Isabel has been reviewed by, for instance, Tolman et al. (2005). The main purpose of the present study is to assess the accuracy of these two wave models regarding the maximum significant wave height, the associated spectral peak wave period, and the time of occurrence for each storm event at a given buoy location. The model results used here are taken from the monthly hindcast data produced by NCEP. They

* Marine Modeling and Analysis Branch Contribution Number 283.

Corresponding author address: Yung Y. Chao, NCEP/EMC/MMAB, 5200 Auth Rd., Camp Springs, MD 20746.
E-mail: yung.chao@noaa.gov

DOI: 10.1175/2010WAF2222309.1

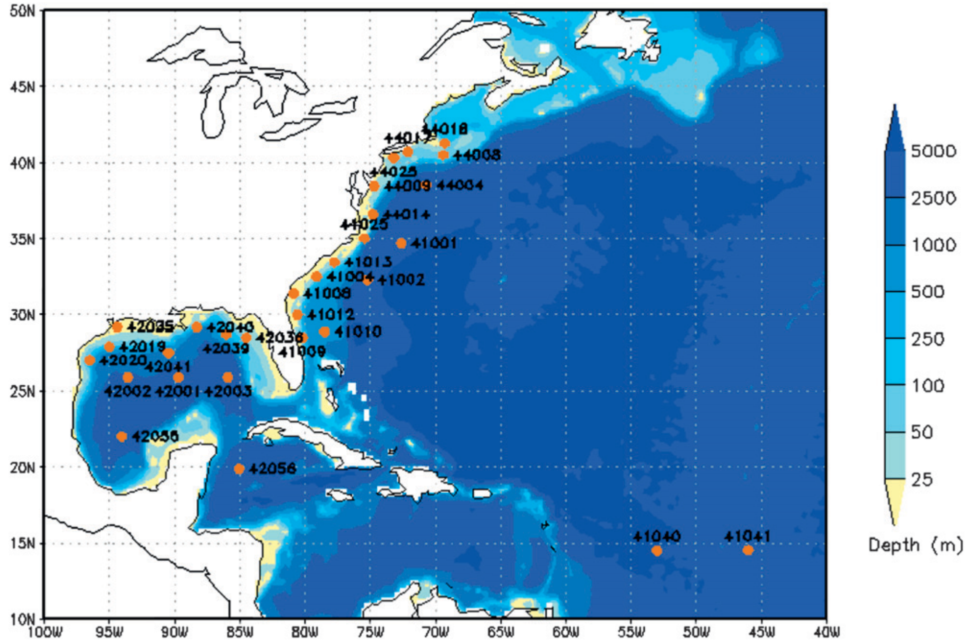

FIG. 1. Locations of NDBC buoys used in the model validation.

represent operational hindcast model data consistent with the operational real-time products of NCEP and do not include any additional tuning or model modifications.

2. Models and data

Wave model data are generated by two operational regional wave models (WNA and NAH). These two models have identical model physics, spatial resolutions, and domains. The domain covers an area of 0°–50°N, and 30°–98°W, involving the North Atlantic basin, the Gulf of Mexico and the Caribbean Sea. The grid resolution is $0.25° \times 0.25°$ in latitude and longitude. Both models obtain boundary data from NCEP's global wave model, which has a resolution of $1.00° \times 1.25°$ in latitude and longitude. The model physics consist of the default model settings of WAVEWATCH III version 2.22, as described in detail in Tolman (2002b). The difference between the two models lies in their input winds. The WNA model is driven solely with wind obtained from the NCEP Global Forecast System (GFS) atmospheric model, previously known as the Medium-Range Forecast (MRF) or Aviation (AVN) model (Caplan et al. 1997). For the NAH model, high-resolution wind fields generated hourly at NCEP by the Geophysical Fluid Dynamics Laboratory (GFDL) hurricane model are blended into the GFS wind field. For the 2005 hurricane season, the GFS model's horizontal resolution is T382, approximately 30 km, and the vertical resolution is 64 layers (see the history of upgrades to GFS online at http://www.emc.ncep.noaa.gov/modelinfo/). The lowest atmospheric level is at a pressure of 997.3 hPa. Since the GFDL hurricane prediction model became operational at NCEP in 1995, it has undergone substantial modifications and improvements (Bender et al. 2007). The 2005 GFDL model has a movable three-nest grid configuration. The horizontal resolution of the outermost nest is ½°, covering an area of $75° \times 75°$ in latitude–longitude. The size of the inner finer mesh is $1/6°$, covering an area of $11° \times 11°$ in latitude–longitude. The finest center core mesh size is $1/12°$, covering an area of $5° \times 5°$ aligned to a single storm center. The number of vertical levels in the GFDL model is 42. The lowest sigma level is 996 hPa.

The 2005 GFS model provides forecast wind fields at 3-h intervals for the first 180 h and then at lower spatial and temporal resolutions for up to 16 days for each operational cycle run. The GFDL model, on the other hand, provides forecast wind fields hourly up to 126 h only. To blend with GFDL wind fields, hourly GFS wind fields are generated by interpolation. The required wind field to be used in the wave models is at a 10-m height. Thus, the lowest sigma-level winds given by the GFS and GFDL models are converted to 10-m heights before blending and interpolating to a uniform $0.25° \times 0.25°$ wave model grid. The blending scheme is described in detail in Chao et al. (2005). The wave models operationally run four cycles per day. Each cycle generates a 6-h hindcast that precedes the actually forecasts. The forecasts extend up to 180 and 126 h for the WNA and

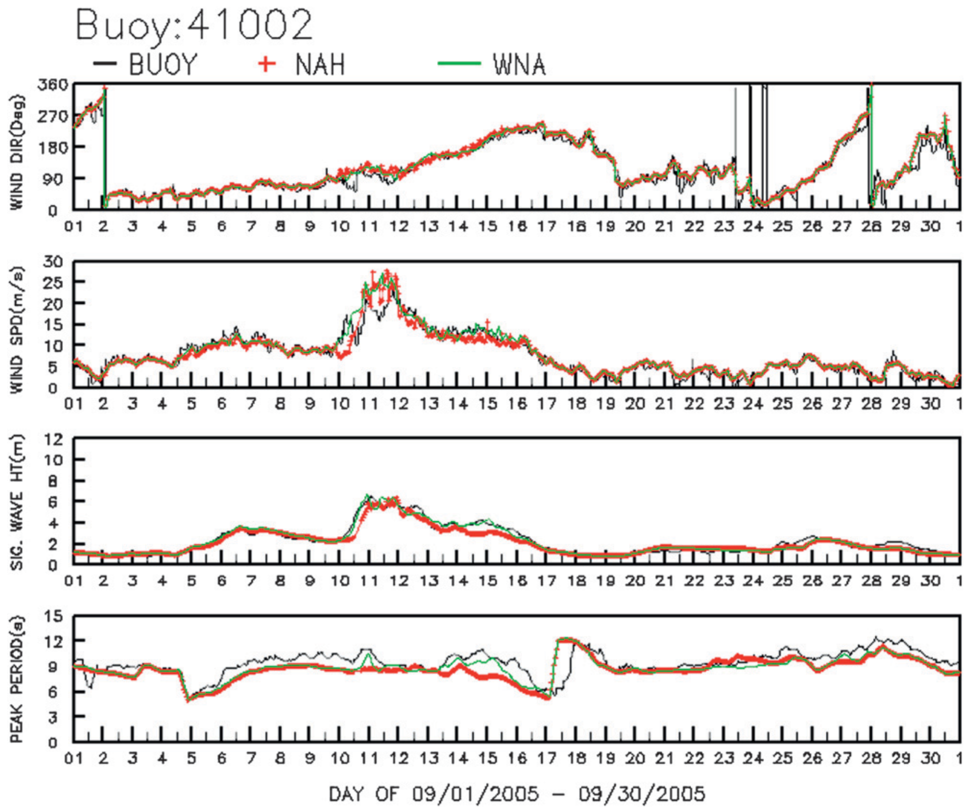

FIG. 2. (bottom to top) Monthly time series of the measured (black) and predicted (NAH, red; WNA, green) spectral peak periods, significant wave heights, wind speeds, and wind directions at buoy 41002, September 2005.

NAH models, respectively. In this study only hindcast wave data are used. It should be noted that the term ''hindcast'' used in this paper has a slightly different connotation from the conventional (engineering) definition. Wave hindcasts in the WNA model driven exclusively with GFS winds are generated using 3-hourly analyses from GFS's Global Data Assimilation System (GDAS; see e.g., Caplan et al. 1997) for a 6-h period preceding the current cycle's UTC time stamp and are used to provide initial conditions for the wave model real-time forecast. Unlike the GFS, the GFDL model does not include a data assimilation system for the initialization of the model forecast. Thus, the NAH model hindcasts are generated using the GFS analysis winds blended with GFDL forecast winds for the 0–4-h range from the previous cycle (−6 to −2-h range in the current cycle). Wind input for NAH at the −1-h time of the current cycle is obtained by interpolating the −2-h winds with the blended GFS–GFDL 0-h nowcast. Although this may seemingly lead to lower quality winds being used for the NAH model hindcast, the higher-resolution winds available from the GFDL short-range forecast (0–6 h) may compensate for deficiencies in the lower-resolution GFS–GDAS analyses.

Quality controlled wave data for model validation were obtained from the NDBC Web site (http://www.ndbc.noaa.gov/historical_data.shtm). Figure 1 shows the locations of all operational NDBC buoys that provide measured data used in the present study. The results of predictions made by the NAH and WNA wave models on the grid points surrounding these locations are interpolated to these locations for validation. In the present study, hourly data obtained from buoy measurements and model output, including the wind speed at 10 m above the mean sea level, the wind direction, the significant wave height, and the spectral peak wave period, are used. The spectral peak wave period is the wave period that corresponds to the frequency bin of maximum wave energy in the wave spectrum. In addition, the significant wave steepness fields are calculated from the NAH model for the significant wave heights greater than 2 m. The significant wave steepness is defined here as the ratio of the significant wave height to the wavelength associated with the spectral peak wave period. Since only a limited amount of wave data obtained from altimeters is available for the present study, they are not included.

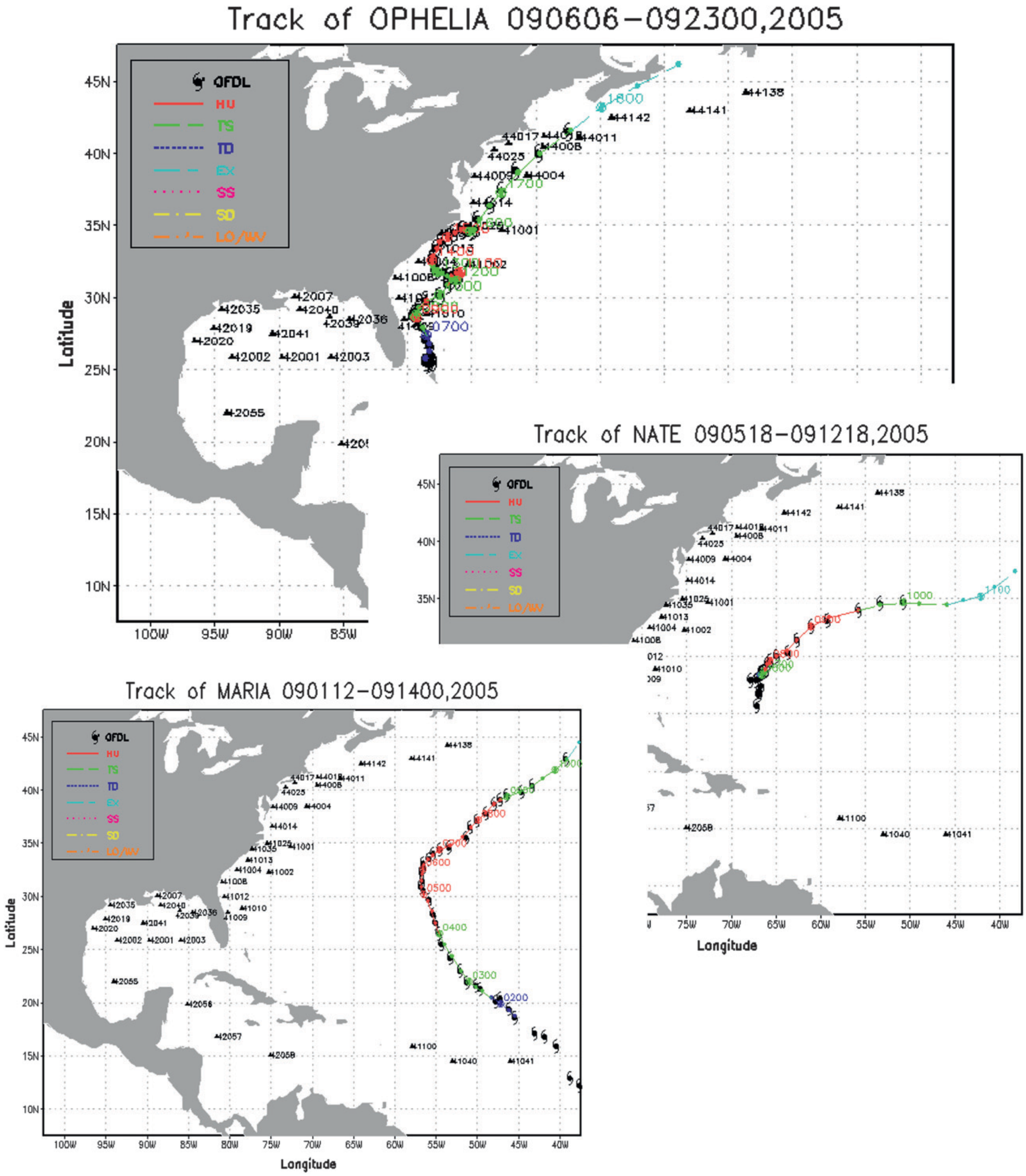

FIG. 3. Best tracks and GFDL model tracks for Hurricanes Maria, Nate, and Ophelia.

3. Identification of the peak significant wave height associated with a tropical cyclone

In this study, we assume that waves appearing at a buoy location must have the significant wave height in a continuous record, peaking up to greater than 2 m in order to be considered as being caused by a tropical cyclone. Furthermore, we assume that the submarine bottom effects on wave height, such as wave refraction and bottom friction, can be ignored in water with a depth

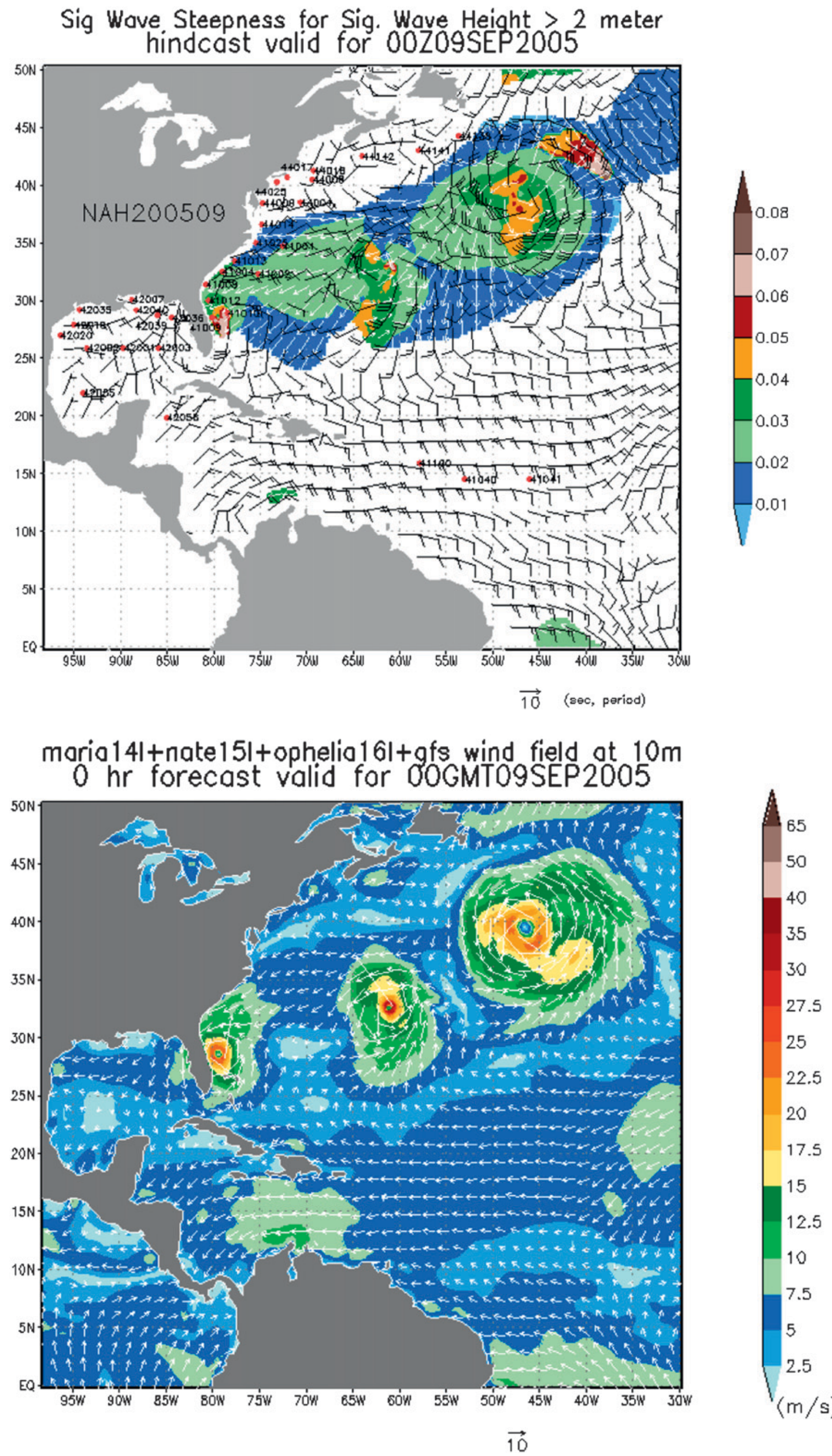

FIG. 4. (top) Wave steepness (for HS > 2 m) and (bottom) blended wind fields (m s^{-1}) while Hurricanes Maria, Nate, and Ophelia coexisted. (bottom) From east to west, Hurricanes Maria, Nate, and Ophelia. Reference arrow at bottom of panels represents 10 m s^{-1} wind speed (bottom), and 10-s peak wave period (top).

TABLE 1. List of tropical cyclones for the wave model validation study.

Tropical cyclone	Cyclogenesis date	Cyclolysis date	Category	Deep-water buoys with the significant wave heights > 2 m
Arlene	8 Jun 2005	12 Jun 2005	TS	42001, 42003, 42039, 42040
Cindy	3 Jul 2005	6 Jul 2005	Category 1	42001, 42003, 42039
Dennis	5 Jul 2005	11 Jul 2005	Category 4	42001, 42003
Emily	11 Jul 2005	21 Jul 2005	Category 4	42001, 42003
Katrina	23 Aug 2005	31 Aug 2005	Category 5	41010, 42001, 42002, 42003, 42039, 42040, 42055
Maria	1 Sep 2005	10 Sep 2005	Category 3	41001, 44004
Nate	5 Sep 2005	10 Sep 2005	Category 1	41002
Ophelia	6 Sep 2005	18 Sep 2005	Category 1	41001, 41002, 41010, 44004
Philippe	17 Sep 2005	24 Sep 2005	Category 1	41040, 41041
Rita	18 Sep 2005	26 Sep 2005	Category 5	41010, 42001, 42002, 42039, 42040, 42055
Stan	30 Sep 2005	5 Oct 2005	Category 1	42001, 42002, 42039, 42055
Tammy	5 Oct 2005	6 Oct 2005	TS	41002, 41010
Wilma	15 Oct 2005	25 Oct 2005	Category 5	41001, 41002, 41010, 41040, 41041, 42001, 42002, 42003, 42039, 42040, 42055, 42056, 42057, 44004
Beta	27 Oct 2005	31 Oct 2005	Category 3	42056, 42057

Note: Buoy numbers shown as 41xxx or 44xxx are in the North Atlantic and as 42xxx are in the Gulf of Mexico–Caribbean Sea (see Fig. 1 for buoy locations).

of greater than 200 m. Consequently, we may use wave data obtained for buoy stations from such locations for storm identification. The procedures used to identify a storm that causes the significant wave height to peak up to a maximum (hereafter called the peak significant wave height) at a given buoy location at a specific time are best described by example. We use data for buoy station 41002 off the Atlantic coast in deep water (depth of 3316 m) during September 2005 for illustration. The example is particularly interesting because of three hurricanes coexisting over the North Atlantic Ocean at one time.

Figure 2 shows hourly time series of observed and predicted wave and wind conditions for September 2005. The plots include the spectral peak wave period, the significant wave height, the wind speed at 10 m above the mean sea level, and the wind direction. There are two significant wave height peaks shown in the second panel from the bottom in Fig. 2. For buoy measurement, the first peak appears at 1300 UTC 6 September and the second peak appears at 2300 UTC 10 September. For the NAH model, the first peak appears at 1600 UTC 6 September and the second peak appears at 0000 UTC 11 September. And for the WNA model, the first peak is at 1500 UTC 6 September and the second peak is at 2300 UTC 10 September. For this example, the significant wave height peaks predicted by the WNA model occur an hour earlier than the peaks predicted by the NAH model. It should be noted that we are interested in the quantity of the spectral peak wave period of the wave spectrum, from which the calculated significant wave height appears to be a peak in the time series. These two quantities are "simultaneous" in time. We are not interested in correlating the significant wave height maximum of the significant wave height time series with the maximum value of the spectral peak wave period time series. The occurrence of a peak on the spectral peak wave period time series is not necessarily associated with (or related to) the considered peak on the significant wave height time series.

Five named hurricanes appeared one after another in the western North Atlantic Basin during September 2005. Three of these storms existed when peaks in the significant wave height occurred at buoy station 41002. They are Hurricane Maria (category 3) during 1–10 September, Hurricane Nate (category 1) during 5–10 September, and Hurricane Ophelia (category 1) during 6–18 September. Figure 3 shows the track positions of the GFDL hurricane model at 6-h intervals. The best tracks (the verified tracks) for these hurricanes are also plotted at 6-h intervals based on data available from the National Hurricane Center (NHC) archive of the 2005 Atlantic hurricane season. The date of the best-track position at 0000 UTC is indicated along the path. The development of a storm's intensity along the track is indicated by segments of different colors and line types. They might involve a tropical low/wave (LO/WV), subtropical depression (SD), subtropical storm (SS), extratropical system (EX), tropical depression (TD), tropical storm (TS), or hurricane (HU). It can be observed from Fig. 3 that the GFDL hurricane model tracks are virtually the same as the best tracks. This is because data for the initialization of the GFDL model is derived from the result of data assimilation (involving the use of observed data) for the GFS model initialization processes (i.e., in the hindcast model).

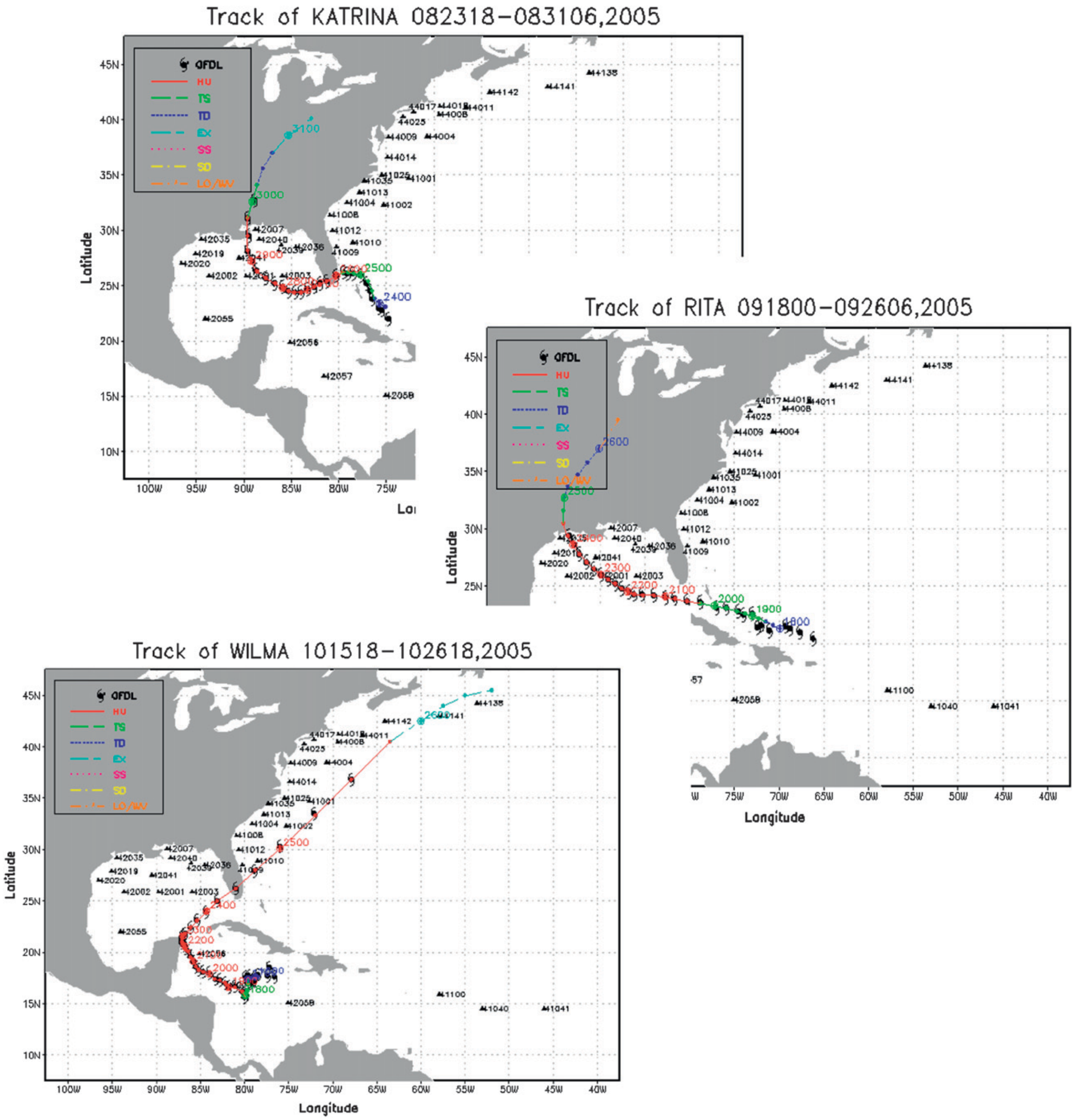

FIG. 5. Best tracks and GFDL model tracks for Hurricanes Katrina, Rita, and Wilma.

To determine which one of these hurricanes causes the significant wave height to reach a maximum, the following steps have been taken. We begin with the construction of the wind fields and the wave steepness fields covering the life cycle of tropical cyclone under study. Figure 4 is an example showing the patterns of the wind (bottom panel) and wave steepness (top panel) fields when three hurricanes coexist over the North Atlantic Basin. The shaded wave steepness contours are given only for the region where the significant wave height is greater than 2 m. Within the shaded area, the hurricane wind bars and the direction of the spectral peak wave period are presented. The direction of the spectral peak period is considered to be the representative wave direction.

We then visually examine sequential plots of the vector wind field and model-derived significant wave steepness patterns. We first observe the pattern orientation

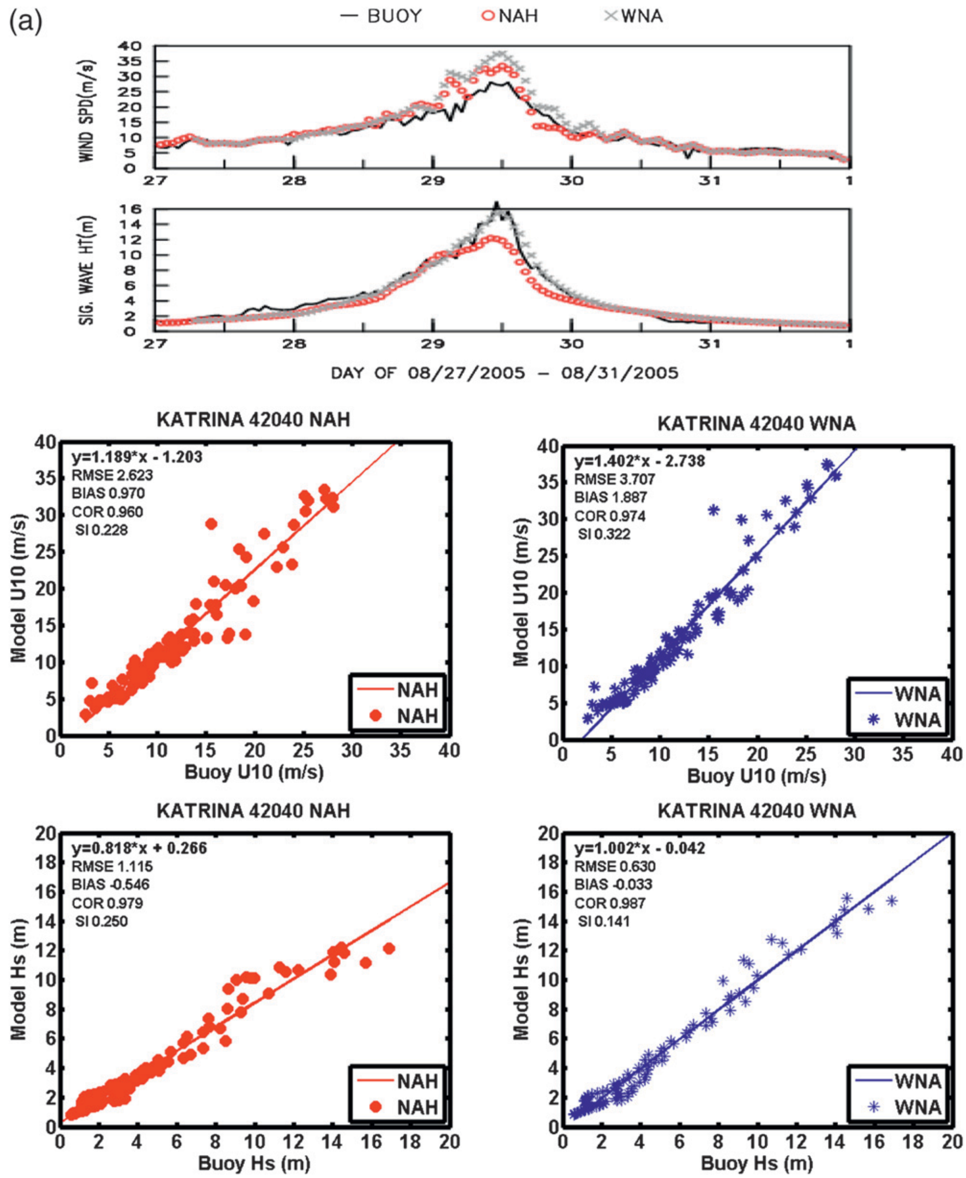

FIG. 6. (a) (top two panels) Buoy measurements (black) and time history and (bottom four panels) error statistics of the NAH- (red) and WNA- (blue) predicted Hs and U_{10} for Hurricanes Katrina at buoy 42040. (b)–(d) As in (a), but for Hurricanes: Ophelia at buoy 41002, Rita at buoy 42001, and Wilma at Buoy 42056.

and the extent of the wind and wave steepness fields to see if they are moving toward the buoy location (The animation of the significant wave steepness fields at 3-h intervals is very helpful.) If these fields indeed move toward and eventually cover the buoy location, we then examine whether the directional variation of the wind and wave inside the shaded wave steepness areas is consistent with the time series of the wind and wave direction at the buoy location as shown in Fig. 2. It is a tedious, time-consuming, trial-and-error process. But in this manner, the storm that causes the wave height to peak up to a maximum at the given location and time can be identified eventually. For the case of buoy station 41002 during September 2005, it is found that the first wave height peak shown in Fig. 2 is identified to be caused by Hurricane Nate and the second wave height peak is identified to be caused by Hurricane Ophelia.

The same procedure is applied to all of the tropical cyclones that occurred during 2005 for all of the available deep-water buoy stations. Table 1 list the names of the tropical cyclones and the deep-water buoy locations where the significant wave heights peak at more that 2 m

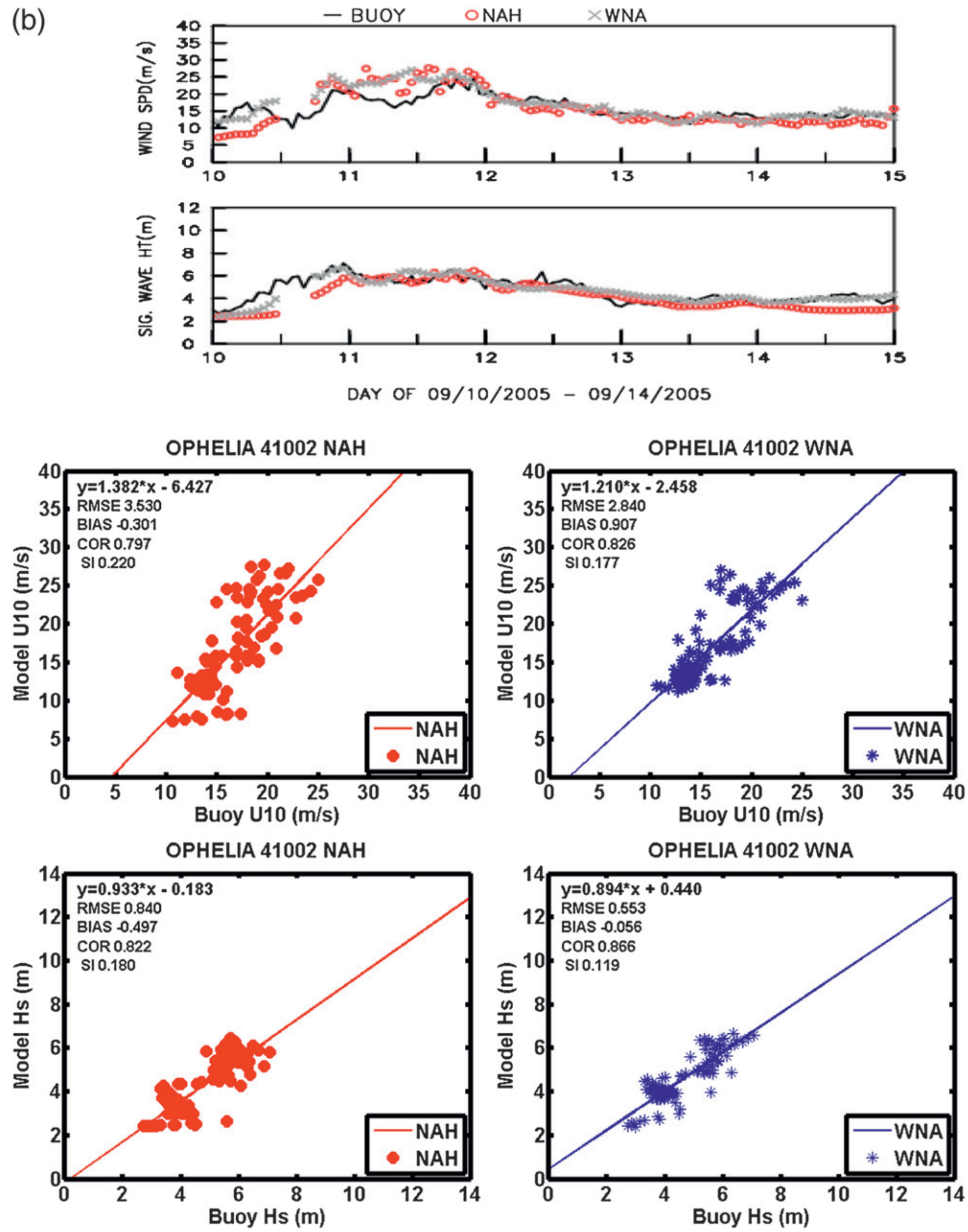

FIG. 6. (*Continued*)

are observed and/or modeled. A total of 14 storms (among 28 for the whole 2005 hurricane season) are identified to have a peak significant greater than 2 m at one or more than one of 14 deep-water buoys. For buoy stations in shoaling waters (buoy stations in the water depths less than or equal to 200 m), the peak conditions associated with a specific storm event are inferred from nearby deep-water buoy stations. Detailed one-to-one comparisons of the significant wave height, peak period, and the time of occurrence between buoy measurements and model predictions are given in appendixes A and B for the Atlantic basin and the Gulf of Mexico, respectively. In these appendixes, 16 additional shoaling water buoy sites are included.

4. Model performance

As previously mentioned, our main objective in this study is to evaluate the performance of the WNA and NAH models for the western North Atlantic basin and the Gulf of Mexico–Caribbean Sea, respectively, in predicting the tropical cyclone–generated maximum

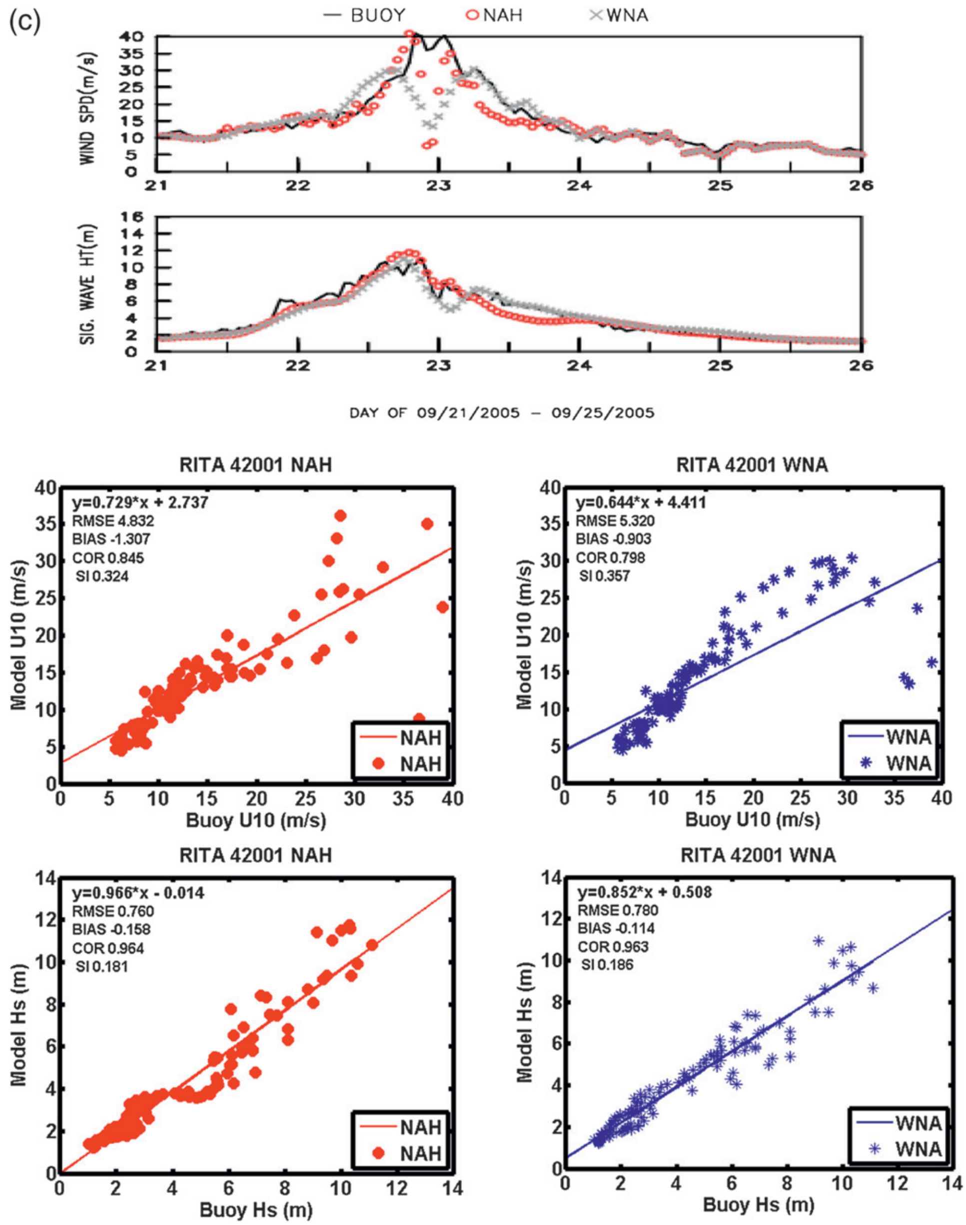

FIG. 6. (*Continued*)

significant wave height, simultaneous spectral peak wave period, and the time of occurrence during the 2005 hurricane season. These two regions are considered separately because the Gulf of Mexico–Caribbean Sea is a semi-enclosed basin while the Atlantic basin is an open ocean. The accuracy of prediction for the two regions might differ due to different geographic constrains on the characteristics of tropical cyclone–induced wind waves. The section is divided to two subsections. Section 4a evaluates the wind speed and the significant wave height predictions for each tropical storm against available buoy observations for 5 days around the evolution of the peak significant wave height. Section 4b then evaluate specifically the performance of the models in predicting the peak significant wave height, the simultaneous wave period, and the time of occurrence.

a. 5-day statistics around the significant wave height peak

We begin with an evaluation of modeled wind speeds and significant wave heights against buoy measurements for four selected storms over a 5-day time span around

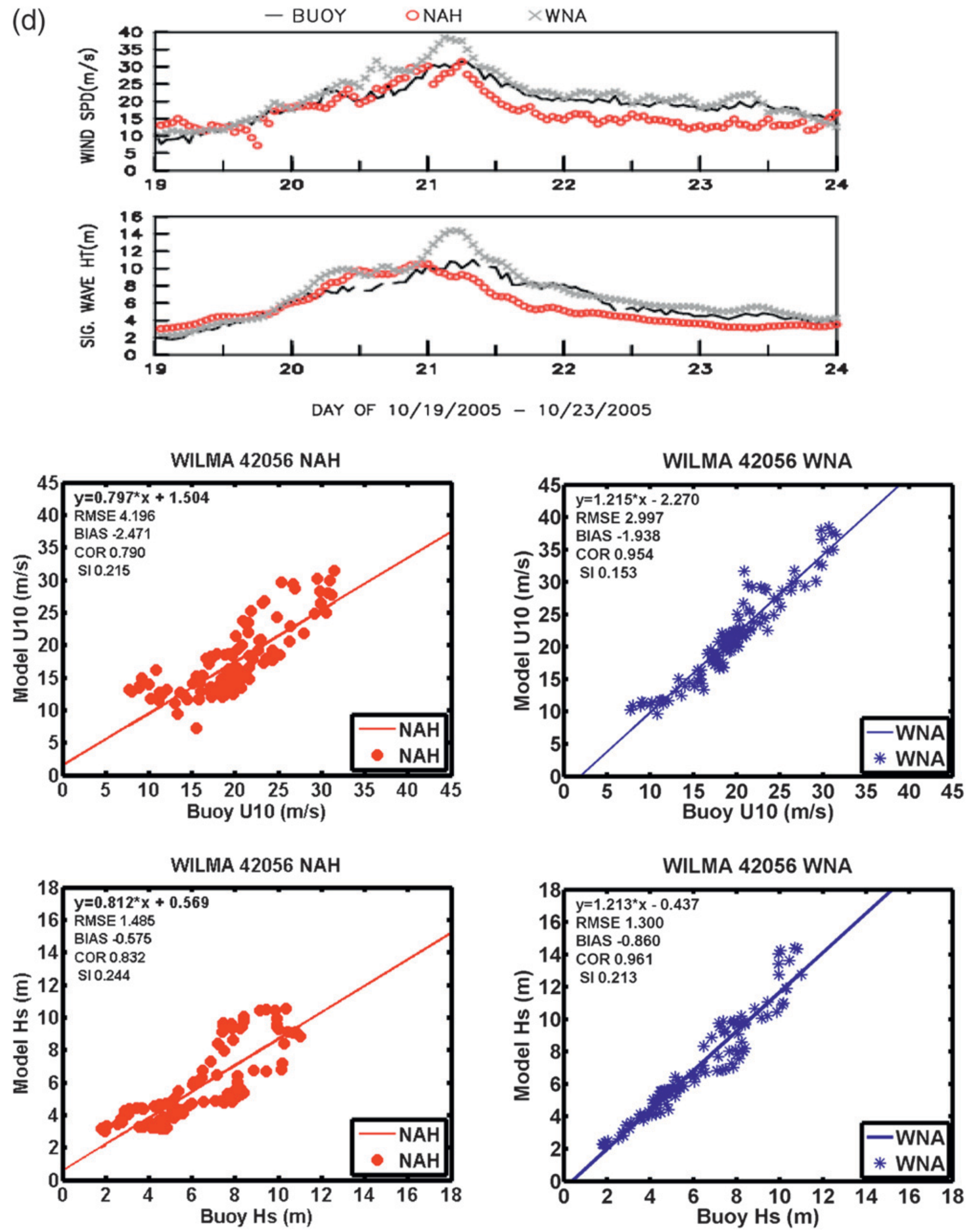

FIG. 6. (*Continued*)

the significant wave height peaks. The selected storms are three category 5 hurricanes (Katrina, Rita, and Wilma) and a category 1 hurricane (Ophelia). Hurricane Ophelia never made landfall but because of its slow movement along the East Coast coastline, it produced sustained high waves for several days (see Fig. 3 for the track of Hurricane Ophelia). Each buoy selected represents the site where the maximum significant wave height peak of the corresponding hurricane was recorded among all of the buoys. Although rather subjective, the selected 5-day time span is assumed to be sufficient to see the rise and fall of the significant wave height around the peak. For each selected storm and buoy site, a total of 120 hourly data points are involved. Figure 5 exhibits the tracks of three category 5 hurricanes. Figures 6a to 6d present the time histories and scatterplots of the wind speeds at 10-m height above the mean seawater level (U_{10}) and the significant height (Hs) caused by Hurricane Katrina at buoy 42040 and Hurricane Rita at buoy 42001 in the Gulf of Mexico, Hurricane Wilma at buoy 42056 in the Caribbean Sea, and Hurricane Ophelia at buoy 41002 in the North Atlantic Basin. Also shown in

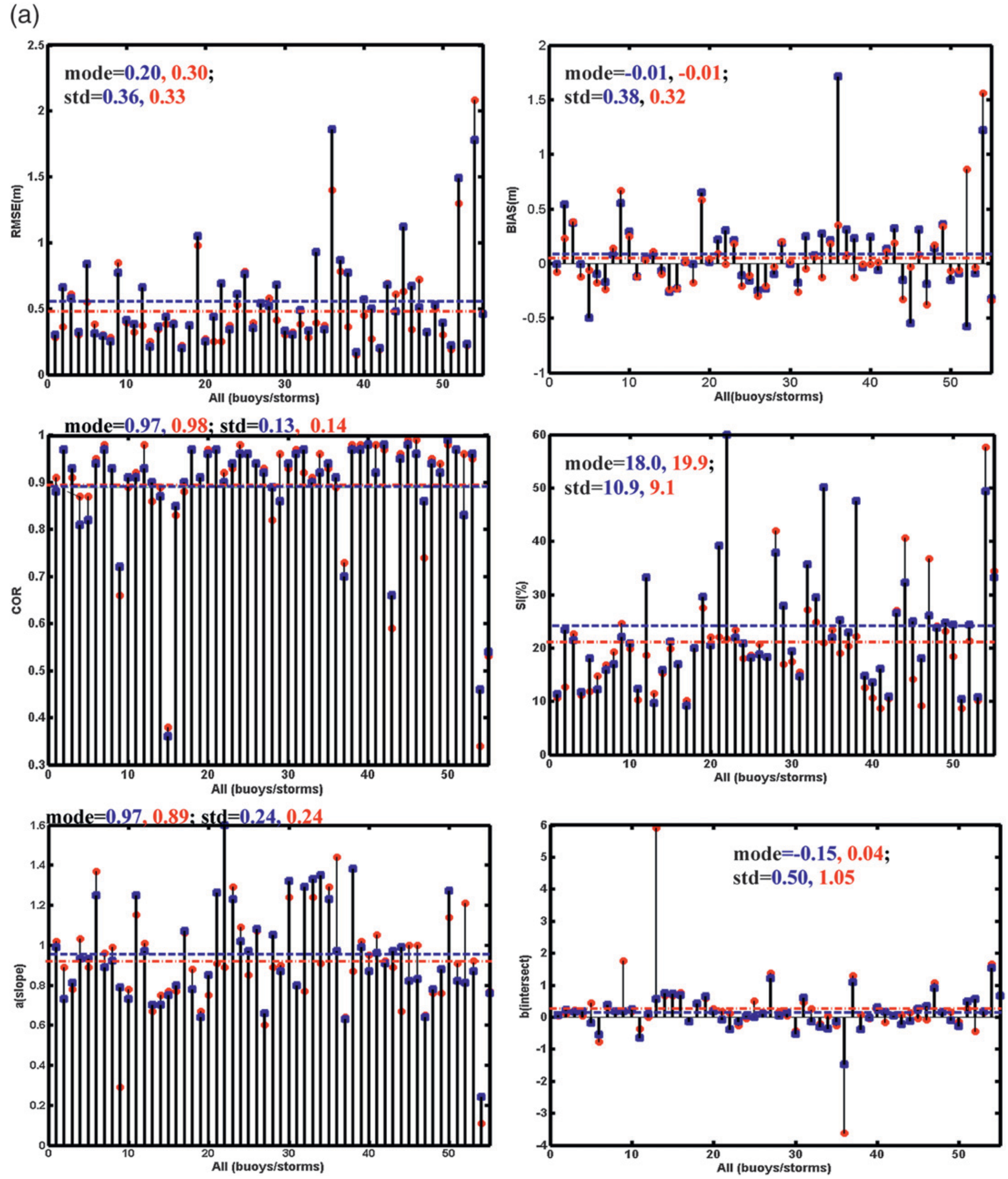

FIG. 7. (a) Error statistics: and linear trends in NAH- (blue) and WNA- (red) predicted Hs for all tropical cyclones at all buoy sites. Dash lines show the mean values: (top) (left) RMSE (right) BIAS; (middle) (left) COR and (right) SI; and (bottom) slope parameters (left) *a* and (right) *b*. (b) As in (a), but for U_{10}.

these figures are the root-mean-square error (RMSE), mean bias (BIAS), correlation coefficient (COR), scatter index (SI), and the linear trend, including the slope and the intersection with an axis. The scatter index is defined as the root-mean-square error normalized by the mean observation.

It can be seen from the time series plots shown in Fig. 6a that for Hurricane Katrina at buoy 42040 during the time period of 0000 UTC 27 August–2300 UTC 31 August, the U_{10} of WNA and NAH are both overpredicted for most of time, especially for WNA near the peak. However, WNA make a much better overall prediction of Hs than NAH, particularly near the peak. The NAH-predicted Hs values are much lower than the measured results. For Hurricane Ophelia at buoy 41002, as shown in Fig. 6b, the slowly moving feature of the hurricane appears in a relatively long duration of U_{10} at around 20 m s^{-1} and Hs of around 6 m for almost

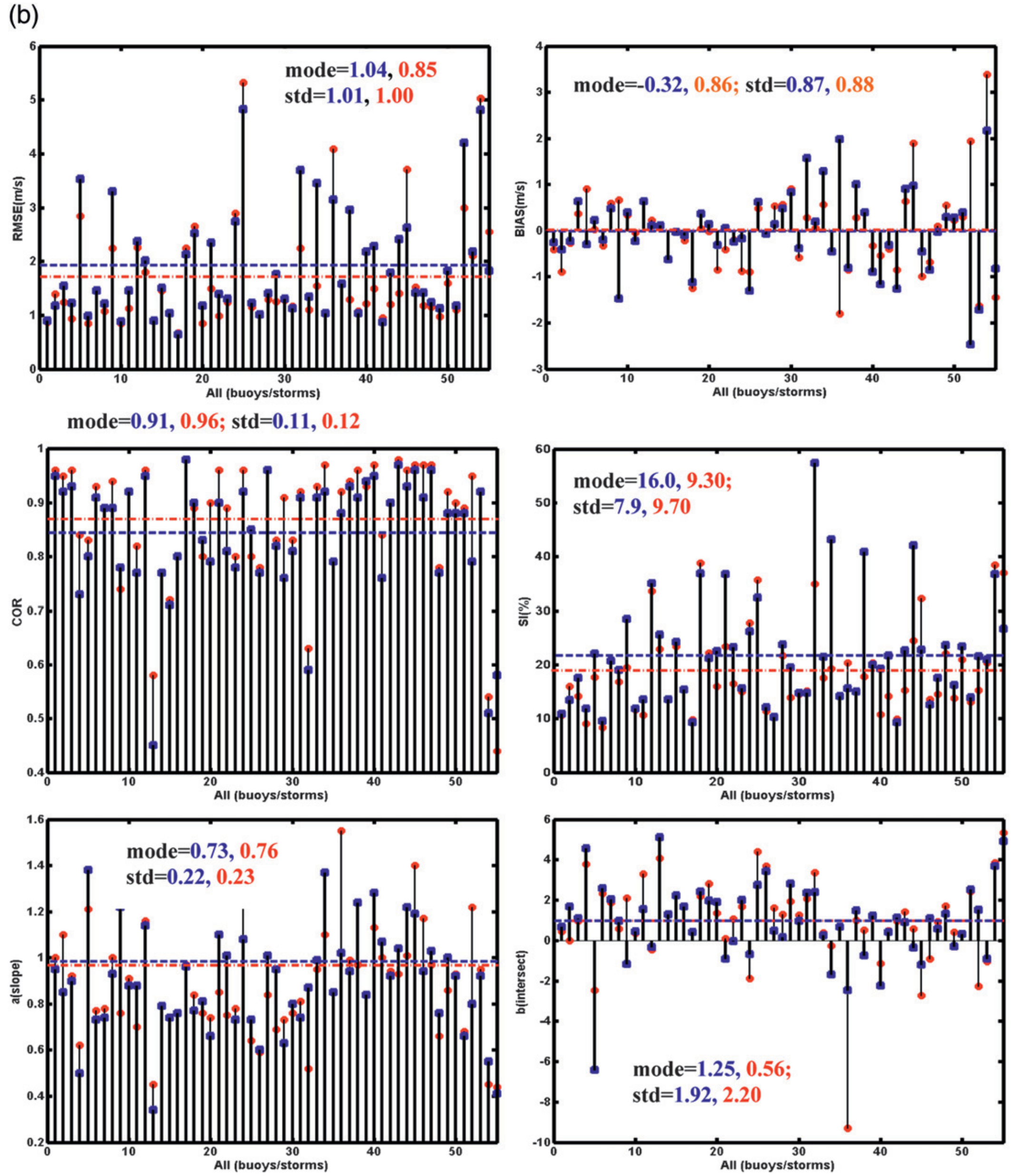

FIG. 7. (*Continued*)

2 days. Again, U_{10} is overpredicted, and Hs is underpredicted by both models. Note that there are six missing data points in the model predictions. Figure 6c shows the ''worst'' wind input associated with Hurricane Rita for the WNA and NAH wave models. As shown in the time evolution of Hurricane Rita, there is a sharp drop in the wind speed. As shown in Fig. 5, the center of Hurricane Rita is in the proximity of the buoy 42001 at about 0000 UTC 23 September. The modeled winds tend to indicate the conditions near the eye of the hurricane, with a rapid change in the wind direction; the wind blows counterclockwise from NNE to NW, to W then to S, within a 5-h period (The time history of the wind directional variations is not shown.) In spite of the substantial discrepancy in the modeled wind speed in comparison with the buoy-measured results, the predicted Hs seems to behave fairly well, underscoring that the modeled Hs's respond to wind speed variations, but do so much more slowly and less dramatically. The results of the NAH and WNA predictions for Hurricane Wilma at buoy 42056, which is located in the Caribbean Sea, are shown in Fig. 6d. As shown in Fig. 6d, the WNA

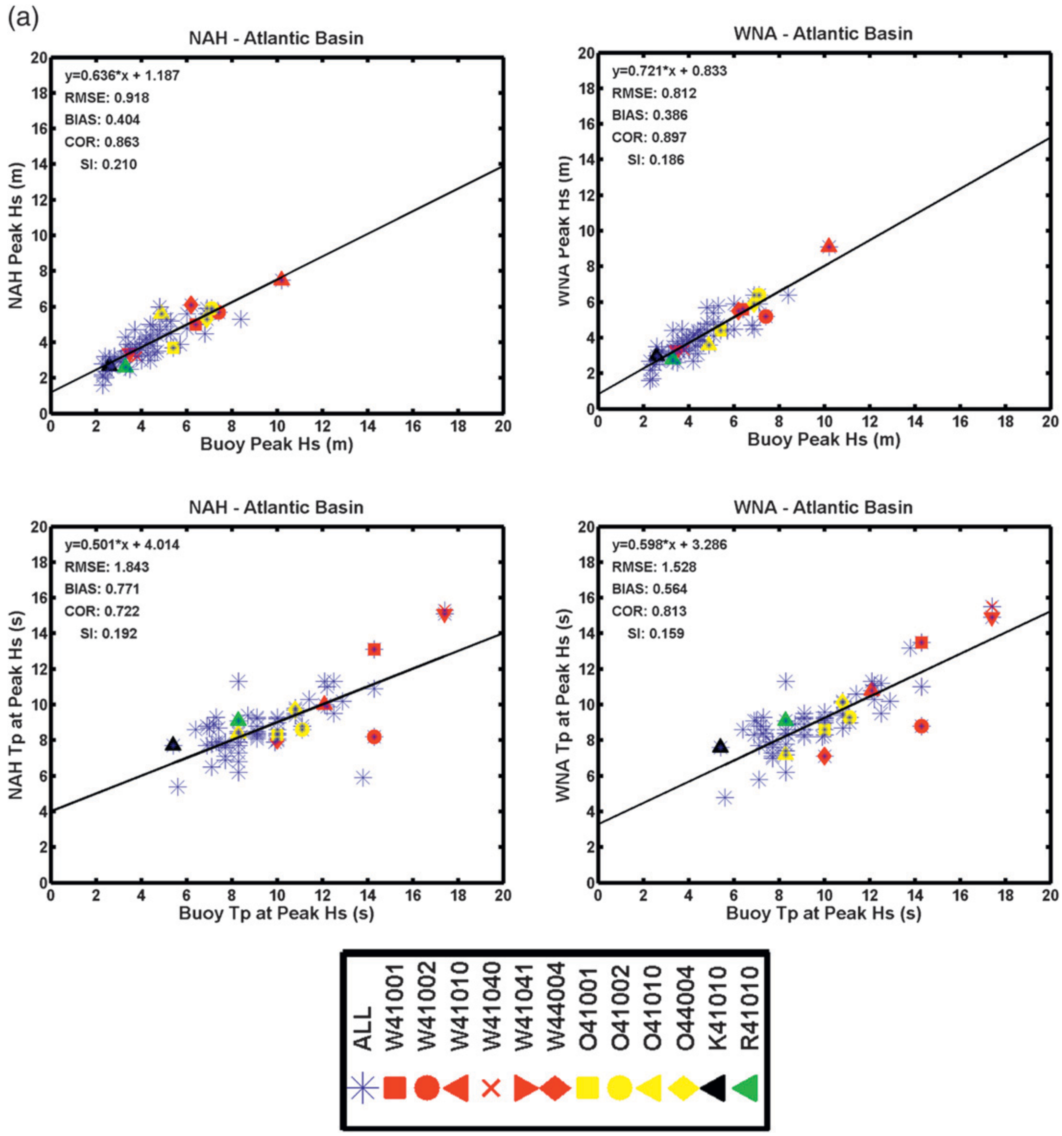

FIG. 8. (a) (top) Scatterplots of the peak Hs and (bottom) the associated spectral Tp for (left) NAH and (right) WNA for the Atlantic basin. Legend at bottom: W, Wilma; O, Ophelia; K, Katrina; R, Rita; followed by buoy ID number. (b) Time lag of the normalized BIAS of (top) the peak Hs and the associated Tp predicted by the (left) NAH and (right) WNA models for the Atlantic basin. In each panel, center lines represent the mean and the outer lines represent the standard deviation. Symbols and colors are as in (a).

model overpredicts U_{10} and Hs around the peak but predicts quite consistently with the observations in the ascending and descending stages. On the other hand, the NAH model predicts the peak Hs near the same height as measured but the time of occurrence is much earlier than was measured even though the modeled maximum wind speed is consistent with the measurement in time and in magnitude. During the descending stage, both U_{10} and Hs are considerably underpredicted. The scatterplots shown in Fig. 6d reveals quantitatively that the NAH-modeled U_{10} and Hs are substantially underpredicted and have negative BIAS, large RMSE, large SI, and low COR, while the linear trend for the WNA-modeled U_{10} and Hs indicates that both are overpredicted but are fairly good in the statistical quantities.

The statistical evaluation of NAH and WNA for the four selected hurricanes at the selected buoys described above has been extended to all selected tropical cyclones and buoys based on the procedure described previously. Figures 7a and 7b summarize the results for Hs and U_{10}, respectively. They are constructed based on data given in appendixes C and D of this paper. The

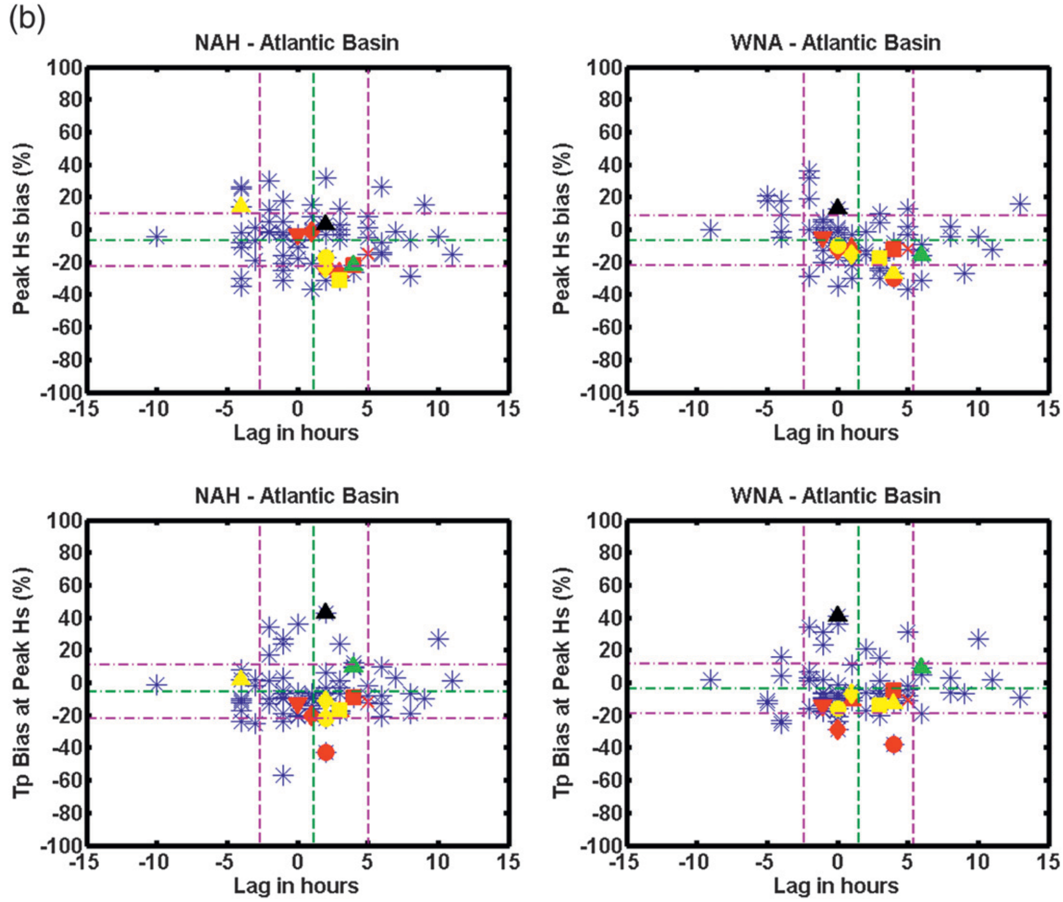

FIG. 8. (*Continued*)

vertical axes for in Figs. 7a and 7b represent one of the statistical quantities described previously [i.e., RMSE, BIAS, COR, SI, and the *a* (slope) and *b* (intersection) terms of the linear trend]. The horizontal axes labeled as ''all (buoys–storms)'' represent the event numbers assigned to the combination of a buoy and identified tropical storms. The event number is assigned according to the combination of the ascending order for the buoy ID number and the alphabetic order for the storm names, beginning with the Atlantic basin followed by the Gulf of Mexico–Caribbean Sea. Thus, the event numbers 1–19 are for the Atlantic basin; for example, 1–3 represent 41001 for Maria, Ophelia, and Wilma, and 17–19 represent 44004 for Maria, Ophelia, and Wilma. The event numbers 20–55 are for the Gulf of Mexico–Caribbean Sea; for example, 20–27 represent 42001 for Arlene, Cindy, Dennis, Emily, Katrina, Rita, Stan, and Wilma, and 54–55 represent 42057 for Wilma and Beta (Hurricane Beta is an exception, as it does not follow the alphabetic order). In each panel, values corresponding to NAH and WNA modeled are shown in blue and red, respectively. The dash lines indicate the mean. Also given in the panels are the mode and the standard deviation (std) of the dataset. The mode in statistics is not necessarily unique, but if it is considered in conjunction with the mean, it can capture important information about what is the value that is most likely to be expected in a discrete dataset. Based on graphs shown in Figs. 6 and 7, the following observations might be made:

1) There are hardly distinct differences visually in the resulting statistics for the Atlantic basin [(case 1) (19)] of the horizontal axis) and the Gulf of Mexico regime [(case 20) (55)] from NAH or WNA modeled Hs or U_{10}.
2) In considering the mean and the mode values given for each of the statistical quantities, both the NAH and WNA models show the following results:
(a) For Hs, the RMSE is about 0.5 m, BIAS is less than 0.1 m, COR is higher than 0.9, and SI is less than 0.2 (20%). The slope of the linear regression line (the *a* term) is slightly less than 0.95, and the intersection

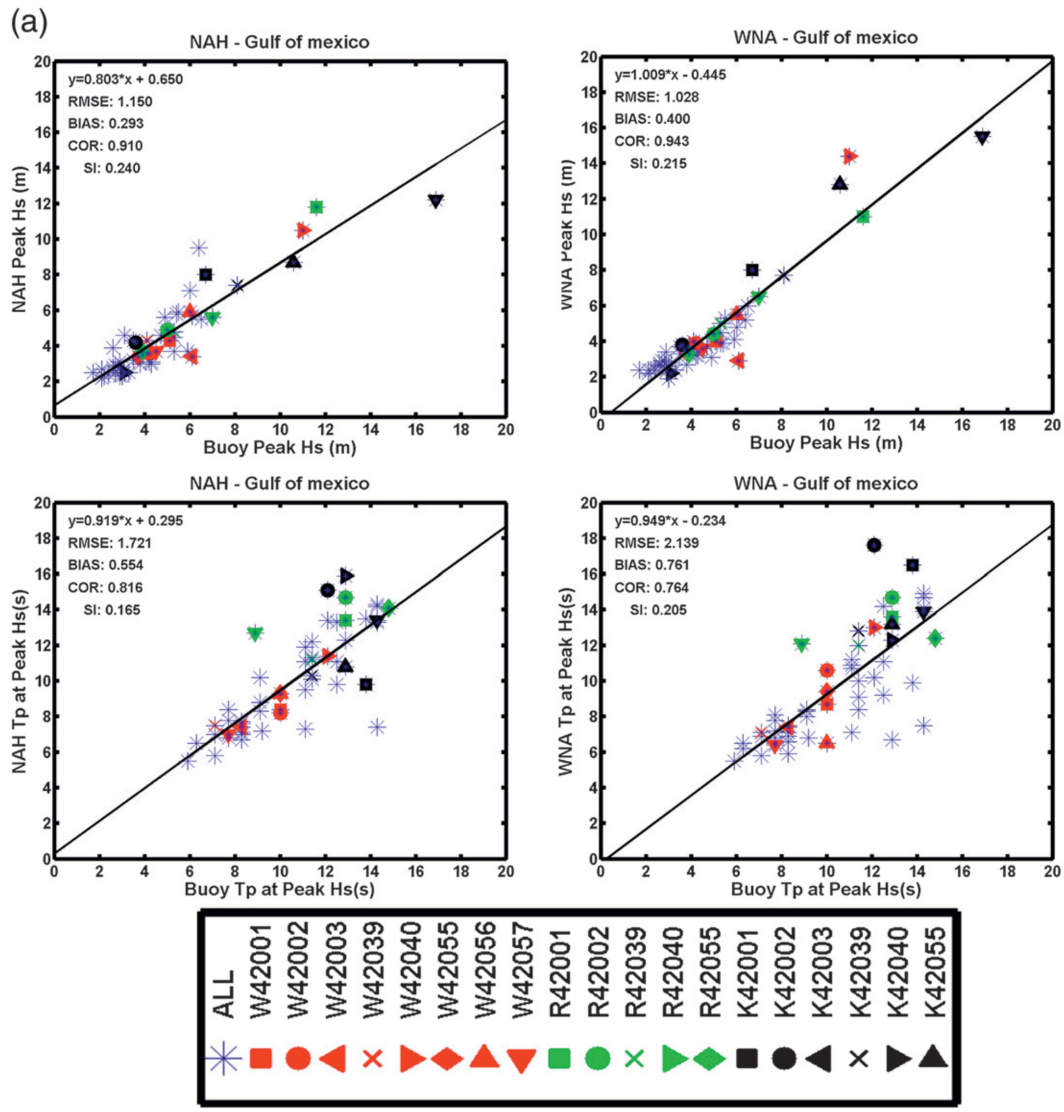

FIG. 9. As in Fig. 8, but for the Gulf of Mexico–Caribbean Sea.

(the b term) is around 0.1 m, indicating that the models tends to underpredict Hs slightly.

(b) For U_{10}, the RMSE is around 2 m s^{-1}, BIAS is near zero but with opposite sign on values for the mode, COR is only slightly above 0.80, and the SI is around 20%. The slope of the linear regression line (a) is nearly 1.0, and the intersection (b) is closer to 1.0 m s^{-1}, indicating the tendency of only slight overprediction of the wind speed.

3) WNA performs comparably to or better than NAH in the overall statistical results.
4) There are a substantial number of outlying points that deviate beyond one standard deviation from the mean in each statistical quantity. No attempt is made to get rid of those extreme values in this paper.
5) The present study clearly shows that the complexity of the hurricane wind and wave fields such that the validation of model performance for one storm event at limited buoys sites is not necessarily applicable to another storm event. An in-depth investigation of the models' performance for each storm scenario regarding the causes of success or failure is important for the improvement of our modeling methodology but is beyond the scope of the present study.

b. *Statistics for the peak significant wave height and the associated wave period*

A major concern in an operational wave forecasting system is the ability to forecast the possible maximum wave height and the time of occurrence at a given

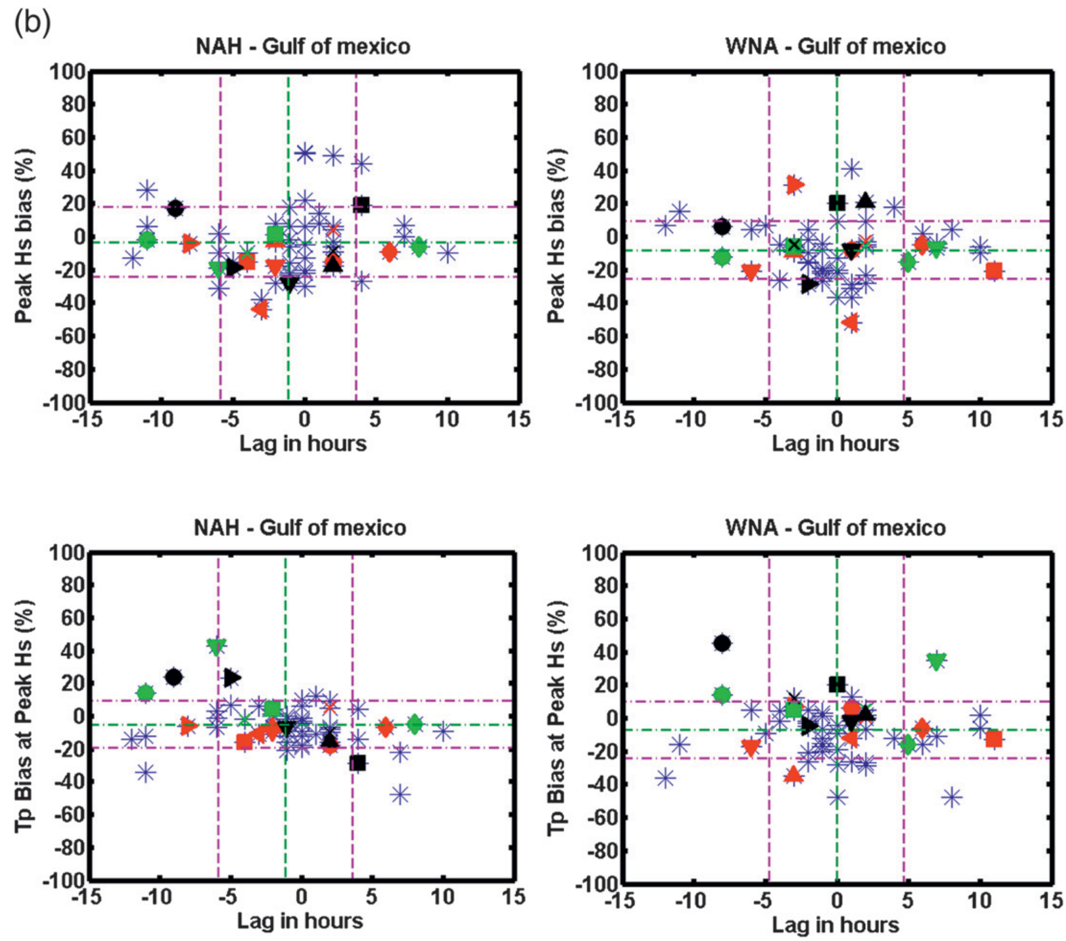

FIG. 9. (*Continued*)

location associated with a given tropical cyclone. The present section evaluates the deviations of the NAH and WNA modeled peak significant wave heights (hereafter, the peak Hs) and the associated spectral peak wave periods (hereafter Tp) and the times of occurrence against buoy measurements.

Figure 8a, containing four panels, depicts the scatterplots of the NAH and WNA modeled peak Hs and Tp for all North Atlantic tropical cyclones, as shown by the asterisk symbol. The database is given in appendix A. In addition, the peak Hs and Tp associated with the hurricanes of particular interest at various buoy sites are plotted with different symbols. In addition, the overall error statistics including root-mean-square error, bias, correlation coefficient, and scatter index, along with the linear trend for all storms and buoys involved, are also presented. Figure 8b shows the normalized bias (difference) between the model predictions and buoy measurements of the peak Hs and Tp as a function of the time lag (difference) in occurrence. The bias is normalized with the buoy measurements and is expressed in percentiles on the vertical axis. The time lag is expressed in hours on the horizontal axis: a negative (or positive) time lag means that the predictions are earlier (or later) than actually observed. The central line in each graph represents the mean value of the labeled quantity, while the outer two lines represent one standard deviation from the mean. Similar graphs for the Gulf of Mexico–Caribbean Sea are depicted in Figs. 9a and 9b based on the dataset given in appendix D.

The scatterplots of the peak Hs for the NAH and WNA models are shown in the top rows of Fig. 8a for the Atlantic basin and in Fig. 9a for the Gulf of Mexico. The plots indicate that the WNA model predictions are slightly better than the NAH model predictions in both the Atlantic basin and the Gulf of Mexico–Caribbean Sea (based on the slope of the regression line). Both models underpredict the peak significant wave height for the Atlantic basin, but predict the wave height for the Gulf of Mexico-Caribbean Sea reasonably well.

Furthermore, for both models, the correlation between observations and the model predictions in the Gulf of Mexico–Caribbean Sea region is better than that in the Atlantic basin. The scatterplots of Tp for the NAH and WNA models (bottom rows in Fig. 8a for the Atlantic and Fig. 9a for the Gulf regions) show results similar to those for the peak Hs. However, Tp has greater bias and a lesser correlation coefficient than does the peak Hs. This is consistent with typical wave model validation results for the spectral peak wave period (Bidlot et al. 2002; Tolman et al. 2005).

The plots of the predicted peak Hs (and Tp) against the predicted time of occurrence for the NAH and WNA models are shown in Fig. 8b for the Atlantic basin and in Fig. 9b for the Gulf of Mexico–Caribbean Sea. As can be observed from the top rows in Figs. 8b and 9b, the normalized bias of the peak Hs is mainly within $\pm 20\%$ but may reach $\pm 30\%$ of the observed value for the Atlantic basin and $\pm 40\%$ for the Gulf of Mexico–Caribbean Sea. The plus sign indicates overprediction while the minus sign indicates underprediction. The mean bias of the peak Hs for both models is approximately -5%. The normalized bias of Tp for both models (bottoms rows in Figs. 8b and 9b) shows similar results to those for the normalized bias of the peak Hs. Thus, the errors are dominated by the model uncertainty (random errors), with the mean bias being comparatively small (less than 5%). The time lag of the model-predicted peak Hs (and the simultaneous Tp) spread considerably, although it was mostly clustered within ± 5 h of the observed peak. On average, both the NAH and WNA models are slightly behind (positive in time lag, on the order of 1–2 h) in predicting the peak Hs and Tp in the Atlantic basin. However, in the Gulf of Mexico–Caribbean Sea, NAH is slightly ahead (negative in time lag) in contrast to WNA, which is on target in time. Note that the observation accuracy of the timing of the peaks is known to be ± 1 h.

5. Discussion

Both the WNA and NAH wave models are capable of providing useful forecast guidance for hurricane-generated waves, with a potential accuracy in the peak significant wave heights that deviates from the observations by roughly 30% within 5 h of the observed time of these maxima. The associated mean biases are much smaller (typically 5%), in comparison to the corresponding random model error. We consider wave model ''hindcasts'' only in this study. Hence, it should be emphasized that the present results merely identify the potential accuracy of the wave model prediction within the framework of the real-time operational environment. It is anticipated that the accuracy of hurricane-associated extreme wave forecasts will be similar depending strongly on the results of the track and wind intensity forecasts of the tropical cyclones that might have occurred. For instance, forecast errors for wave models for Hurricane Isabel in 2003 are discussed in detail in Tolman et al. (2005).

Considering the problems involved with providing accurate hurricane wind nowcasts and forecasts, the method of blending GFS and GFDL model wind fields for the NAH model becomes a subject of concern. In previous hurricane seasons, the NAH model in general has outperformed the WNA model (see Chao et al. 2005). However, for the 2005 season, the models behaved similarly, with arguably better behavior for the WNA model. Within this context, it is important to realize that the wind-blending algorithm was developed almost a decade ago. At that time GFS, previously known as the Medium-Range (MRF) and Aviation (AVN) models, had a grid resolution of about 50 km, which was too coarse to resolve the wind field structure associated with a relatively small hurricane vortex. Thus, the blending algorithm was initiated to incorporate the GFDL hurricane model and take advantage of its high-resolution inner mesh of about 15 km (Chao and Tolman 2000; Chao and Tolman 2001). Since then, has GFS undergone various improvements; among these enhancements was a change in grid resolution to about 30 km in 2005. As a result, GFS was able to provide improved wind forecasts near the hurricane core. More importantly, the resolution of the GFS is now comparable to the resolution of the wave models. Conversely, the resolution of the GFDL model winds is much higher than the resolution of the wave models, and hence the wave models no longer make optimal use of the resolution of the hurricane wind models. It therefore appears to be necessary to increase the spatial resolution of the (hurricane) wave models to effectively use the increased resolution of the hurricane wind models. For this reason, it is necessary to upgrade the hurricane wave model to utilize hurricane winds at or near the native resolution of the hurricane wind fields.

Another reason for the apparently comparable behavior of the WNA and NAH wave models may be the sparsity and a corresponding lack of representativeness of the validation data. This is illustrated in Fig. 10 with results for Hurricane Katrina near landfall at 1200 UTC 29 September. (The hurricane track and the time history of the wind and wave data at buoy station 42040 near the track are shown in Figs. 5 and 6a, respectively.) The top panels in Fig. 10 show the wind fields of the WNA and NAH models. Both models have nearly identical tracks, with the centers of the maximum wind shifted by

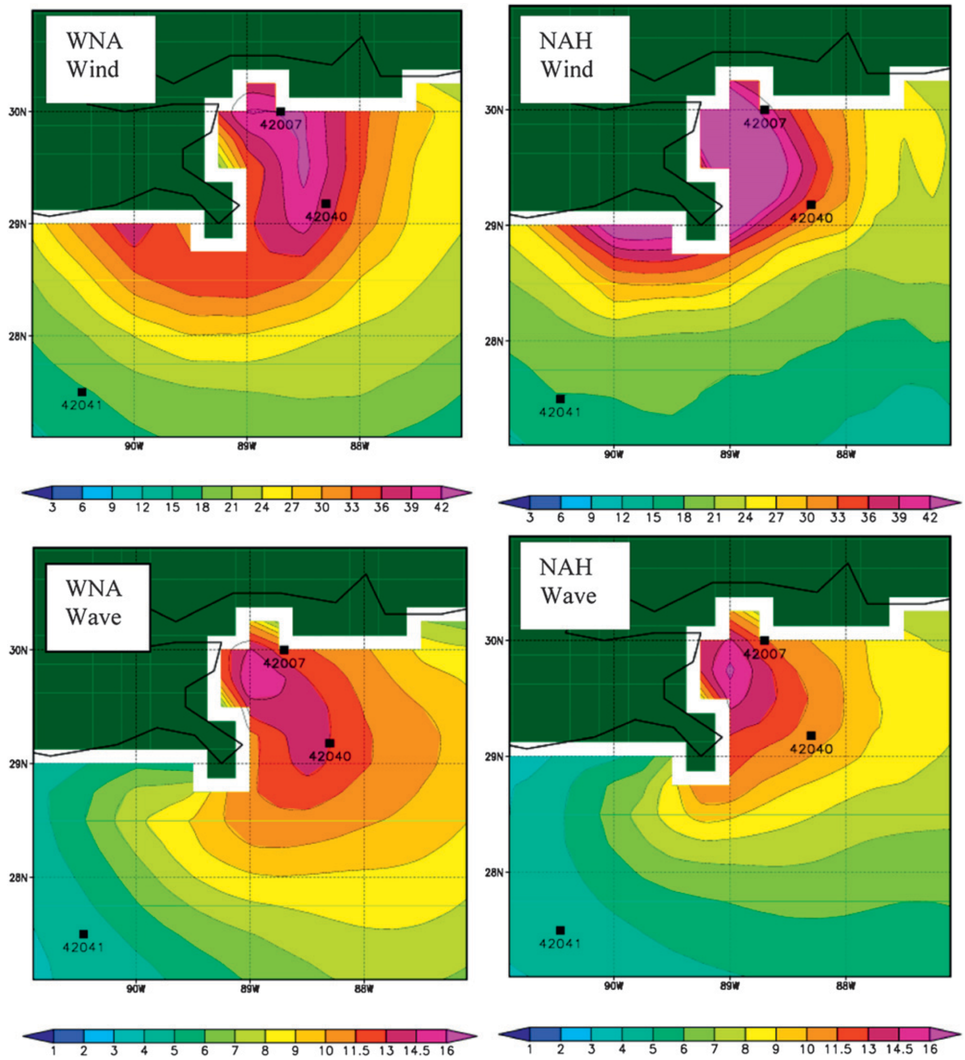

FIG. 10. A comparison of (top) wind and (bottom) wave fields predicted by (left) WNA and (right) NAH for Hurricane Katrina, 1200 UTC 29 Sep.

10–20 km. The NAH winds are more intense with reasonable spatial scales, but are shifted too much to the shallow waters (west). The WNA winds have lower speeds but larger spatial scales. This produces good wind results at the only relevant observation location (buoy 42040), although the wind fields as a whole are less realistic than the NAH wind fields (Chao et al. 2005; Tolman et al. 2005). The corresponding wave height fields (bottom panels in Fig. 10) are also shifted between the models, due to the similar track but different spatial scales of the wind fields. If only buoy data at buoy 42040 were considered, one could easily come to the conclusion that the WNA model is far superior (Fig. 6a). With only the buoy in view in Fig. 10, there is clearly insufficient information to rigorously validate the hurricane wave models, unless the hurricane track is close to the buoys (see Chao et al. 2005; Tolman et al. 2005 for case studies). It therefore appears essential to have routine on-demand wave observations during hurricanes, as was available for Hurricane Bonnie from a Scanning Radar Altimeter (Alves et al. 2004; Wright et al. 2001), to systematically address the accuracy of the hurricane wave models.

Note that the model resolution in 2005 was insufficient to resolve this coastline, and therefore the results from buoy 42007 cannot be expected to be very accurate. Furthermore, wave heights in the shallow waters behind the Chandeleur Islands are obviously unrealistic due to the lack of shallow-water physics in the model and due to the fact that the spatial resolution is too poor to introduce these islands as obstructions. For the 2007 model implementation, the coastal resolution in this area is greatly improved, and surf zone physics (depth-induced breaking) were added to the model (Chawla et al. 2007; Tolman 2008).

6. Conclusions

In this study, we validate NCEP's operational Western North Atlantic regional wave model (WNA) and North Atlantic Hurricane wave model (NAH) against NDBC buoy measurements for more than 20 tropical cyclones (including three category 5 hurricanes) for the 2005 hurricane season. The parameters evaluated include the maximum significant wave height, the corresponding spectral peak period, and the time of occurrence induced by each individual tropical cyclone. The results show that the deviations of the model-predicted wave heights and periods from buoy measurements are essentially within 20% and 30%, respectively, and that the time lags (behind or ahead of observation) on the occurrence of peak wave height are within the 5-h range for both models. Both models show similar patterns of behavior, with model uncertainty dominating the mean model bias, which is typically approximately 5%. Considering that these are operational model results produced in near–real time with no case-specific tuning of the wave models or the wind fields, the biases of both models can be considered to be rather good. Clearly, the model presents useful results for real-time forecasting, but also leaves room for improvement. The similar patterns of behavior in the WNA and NAH models suggests that the hurricane wave model (NAH) no longer optimally uses the higher resolution of the hurricane wind model, suggesting that the spatial resolution of the hurricane wave model needs to be increased to be comparable to that of the hurricane wind model. Note that, generally, better validation of hurricane wave models is greatly hampered by the lack of wave observations with suitable spatial coverage.

The NAH and WNA, as is the case with many other existing third-generation (3G) models, are essentially developed and validated on extratropical wind-forcing regimes characterized with slowly varying wind fields in space and time. The application of such a model in a real-time operational environment for tropical cyclones that are characterized by the rapidly varying extreme surface wind fields along the moving storm track faces various obstacles and uncertainties. The sparsity of measured data is just one of these potential problem areas. We would like to stress that the models are intended as operational models for real-time forecasting. Even if there is insufficient data to do a rigorous statistical analysis of bias versus uncertainty, it appears obvious to us from the present study that a human forecaster using these model data to do his or her work will have to expect the model's uncertainty to be the main problem with the guidance, and that adding a systematic bias correction to the model guidance is a minor correction compared to this uncertainty. Hence, we cannot, based on the sparsity of the data, do an in-depth statistical analysis, but, from the perspective of these being operational forecast models, we do feel confident saying that the biases of the model are small compared to the general uncertainty.

Acknowledgments. The authors thank Janna O'Connor, Arun Chawla, Robert Grumbine, and the anonymous reviewers for their valuable comments and suggestions on our drafts of this manuscript.

APPENDIX A

The Peak Significant Wave Heights (Hs), Simultaneous Spectral Peak Periods (Tp), Times of Occurrence, and Associated Cyclone Names for the Atlantic Basin

Buoy ID (depth)	Buoy Hs (m)	Buoy Tp (s)	Buoy time and date	NAH Hs (m)	NAH Tp (s)	NAH time and date	WNA Hs (m)	WNA Tp (s)	WNA time and date	Name of TC
41001	3.9	9.1	1300 UTC 13 Sep	3.5	8.4	1900 UTC 6 Sep	3.5	8.3	1700 UTC 6 Sep	Maria
(4427 m)	5.4	10	1000 UTC 16 Sep	3.7	8.3	1300 UTC 16 Sep	4.4	8.6	1300 UTC 16 Sep	Ophelia
	4.4	8.3	1200 UTC 15 Oct	4.2	11.3	1200 UTC 15 Oct	4.3	11.3	1200 UTC 15 Oct	SD24
	6.4	14.3	1400 UTC 25 Oct	4.9	13.1	1800 UTC 25 Oct	5.6	13.5	1800 UTC 25 Oct	Wilma
41002	3.6	10	1300 UTC 6 Sep	3.4	8.1	1600 UTC 6 Sep	3.1	8.3	1500 UTC 6 Sep	Nate
(3316 m)	7.1	11.1	2300 UTC 10 Sep	5.8	8.6	0000 UTC 11 Sep	6.4	9.3	2300 UTC 10 Sep	Ophelia
	3.5	9.1	0400 UTC 6 Oct	3.5	9.3	1900 UTC 5 Octr	3.8	9.5	0000 UTC 6 Oct	Tammy
	4.2	8.3	1800 UTC 8 Oct	4.1	8.4	1600 UTC 8 Oct	4.1	8.4	1600 UTC 8 Oct	SD22
	3.8	12.5	2000 UTC 15 Oct	3.3	11.3	2000 UTC 15 Oct	3.4	11.2	2000 UTC 15 Oct	SD24
	7.4	14.3	0800 UTC 25 Oct	5.7	8.2	1000 UTC 25 Oct	5.2	8.8	1200 UTC 25 Oct	Wilma
41004	5.3	10.8	0600 UTC 13 Sep	5.1	9.4	0400 UTC 13 Sep	5.8	8.7	0900 UTC 13 Sep	Ophelia
(34 m)	4.8	10.8	0600 UTC 6 Oct	5.9	9.5	0200 UTC 6 Oct	5.6	9.4	0100 UTC 6 Oct	Tammy

APPENDIX A (*Continued*)

Buoy ID (depth)	Buoy Hs (m)	Buoy Tp (s)	Buoy time and date	NAH Hs (m)	NAH Tp (s)	NAH time and date	WNA Hs (m)	WNA Tp (s)	WNA time and date	Name of TC
41008	3.1	7.7	0900 UTC 7 Sep	3.0	6.9	1000 UTC 7 Sep	2.9	7.0	0900 UTC 7 Sep	Nate
(18 m)	3.7	8.3	0200 UTC 6 Oct	4.6	7.3	2200 UTC 5 Oct	4.4	7.4	2100 UTC 5 Oct	Tammy
	2.4	5.6	0000 UTC 25 Oct	3.1	5.4	0200 UTC 25 Oct	1.6	4.8	0300 UTC 25 Oct	Wilma
41009	4.2	9.1	1300 UTC 8 Sep	4.3	8.5	1600 UTC 8 Sep	2.6	8.9	1800 UTC 8 Sep	Nate
(42 m)	3.5	8.3	0800 UTC 20 Sep	2.4	6.8	1600 UTC 20 Sep	2.5	7.8	1700 UTC 20 Sep	Rita
	4.7	7.2	0700 UTC 5 Oct	3.5	8.9	0600 UTC 5 Oct	3.7	8.8	0600 UTC 5 Oct	Tammy
	6.0	9.9	2000 UTC 24 Oct	5.5	7.9	2000 UTC 24 Oct	5.9	8.2	1900 UTC 24 Oct	Wilma
41010	2.6	5.4	1700 UTC 25 Aug	2.6	7.7	1900 UTC 25 Aug	2.9	7.6	1700 UTC 25 Aug	Katrina
(872 m)	4.9	8.3	0900 UTC 9 Sep	5.5	8.4	0500 UTC 9 Sep	3.5	7.2	1300 UTC 9 Sep	Ophelia
	3.3	8.3	0900 UTC 20 Sep	2.5	9.1	1300 UTC 20 Sep	2.7	9.1	1500 UTC 20 Sep	Rita
	4.4	10	0700 UTC 5 Oct	4.4	9.3	0800 UTC 5 Oct	4.3	9.2	0700 UTC 5 Oct	Tammy
	10.2	12.1	2200 UTC 24 Oct	7.5	10.0	0100 UTC 25 Oct	9.0	10.8	2300 UTC 24 Oct	Wilma
41012	4.2	10	0900 UTC 8 Sep	3.8	8.3	0500 UTC 8 Sep	4.2	8.6	0900 UTC 8 Sep	Ophelia
(38 m)	4.5	10	1500 UTC 5 Oct	4.8	8.4	1600 UTC 5 Oct	4.3	9.1	1600 UTC 5 Oct	Tammy
	2.3	8.3	0000 UTC 14 Oct	2.1	6.2	2100 UTC 13 Oct	2.1	6.2	2000 UTC 13 Oct	SD22
	4.4	7.7	2100 UTC 24 Oct	4.9	7.8	0000 UTC 25 Oct	3.5	7.3	0000 UTC 25 Oct	Wilma
41013	3.3	7.7	0300 UTC 7 Sep	3.1	7.7	1700 UTC 6 Sep	3.3	7.8	1800 UTC 6 Sep	Ophelia
(24 m)	3.3	6.4	1000 UTC 6 Oct	4.3	8.6	0800 UTC 6 Oct	4.3	8.6	0800 UTC 6 Oct	Tammy
	3.4	7.1	0600 UTC 25 Oct	3.9	6.5	0700 UTC 25 Oct	3.1	5.8	0500 UTC 25 Oct	Wilma
41025	4.3	7.4	0800 UTC 6 Sep	3.3	7.9	1000 UTC 6 Sep	3.4	8.2	0900 UTC 6 Sep	Maria
(68 m)	4.6	6.9	1900 UTC 11 Sep	3.4	7.7	2300 UTC 11 Sep	3.9	8.3	2100 UTC 11 Sep	Ophelia
	4.7	7.0	1600 UTC 8 Oct	4.4	8.7	1900 UTC 8 Oct	4.5	9.1	2100 UTC 8 Oct	Tammy
	2.8	12.2	1800 UTC 14 Oct	3.2	11.0	0300 UTC 15 Oct	3.2	11.1	0700 UTC 15 Oct	SD22
	4.4	13.8	1600 UTC 25 Oct	3.0	5.9	1500 UTC 25 Oct	3.0	13.2	1700 UTC 25 Oct	Wilma
41040	3.3	7.7	1900 UTC 17 Sep	2.6	7.1	2000 UTC 17 Sep	2.7	7.0	2200 UTC 17 Sep	Philippe
(4572 m)	3.8	17.4	1700 UTC 16 Oct	3.2	15.3	2200 UTC 16 Oct	3.3	15.5	2200 UTC 16 Oct	Wilma
41041	2.3	7.1	1200 UTC 15 Sep	2.8	7.8	1800 UTC 15 Sep	2.7	7.7	1000 UTC 15 Sep	Philippe
(3353 m)	3.5	17.4	1900 UTC 16 Oct	3.0	15.0	1900 UTC 16 Oct	3.0	15.0	1800 UTC 16 Oct	Wilma
44004	2.7	7.7	0000 UTC 6 Sep	2.7	7.1	0500 UTC 6 Sep	2.7	7.1	0500 UTC 6 Sep	Maria
(3182 m)	6.9	10.8	0600 UTC 17 Sep	5.3	9.7	0800 UTC 17 Sep	5.8	10.1	0700 UTC 17 Sep	Ophelia
	3.9	8.3	0600 UTC 9 Oct	3.8	8.5	1300 UTC 9 Oct	3.9	8.6	1400 UTC 9 Oct	SD22
	7.1	12.9	1900 UTC 13 Oct	5.7	10.2	1900 UTC 13 Oct	5.8	10.2	1900 UTC 13 Oct	SD24
	6.2	10	0600 UTC 25 Oct	6.1	8.0	0700 UTC 25 Oct	5.4	7.1	0600 UTC 25 Oct	Wilma
44008	5.7	10.8	1300 UTC 17 Sep	3.9	9.8	1500 UTC 17 Sep	4.4	10.2	1400 UTC 17 Sep	Ophelia
(63 m)	3.5	9.1	1500 UTC 9 Oct	3.5	8.8	1800 UTC 9 Oct	3.6	9.2	1800 UTC 9 Oct	SD22
	5.1	11.4	1700 UTC 14 Oct	5.3	10.3	1500 UTC 14 Oct	5.3	10.6	1600 UTC 14 Oct	SD24
	8.4	10	1300 UTC 25 Oct	5.3	8.6	1400 UTC 25 Oct	6.3	9.3	1600 UTC 25 Oct	Wilma
44009	2.3	8.3	0900 UTC 6 Sep	2.1	7.7	1700 UTC 6 Sep	2.2	7.8	1700 UTC 6 Sep	Nate
(28 m)	3.1	8.3	0000 UTC 9 Oct	2.9	7.9	2300 UTC 8 Oct	3.1	7.8	2300 UTC 8 Oct	SD22
	4.5	6.9	0600 UTC 14 Oct	3.7	8.8	0500 UTC 14 Oct	3.9	9.1	0500 UTC 14 Oct	SD24
	6.9	8.4	1200 UTC 25 Oct	5.5	8.2	0900 UTC 25 Oct	4.4	8.3	1200 UTC 25 Oct	Wilma
44014	2.8	7.7	0100 UTC 6 Sep	3.0	7.6	0600 UTC 6 Sep	3.1	7.6	0600 UTC 6 Sep	Nate
(48 m)	4.0	7.3	1200 UTC 16 Sep	2.9	7.9	1600 UTC 16 Sep	3.3	8.4	1500 UTC 16 Sep	Ophelia
	4.2	9.1	2200 UTC 8 Oct	3.9	8.5	2200 UTC 8 Oct	4.0	8.6	2100 UTC 8 Oct	SD22
	3.8	14.3	0100 UTC 15 Oct	3.7	10.9	2100 UTC 14 Oct	3.7	11.0	2100 UTC 14 Oct	SD24
	5.1	9.1	0600 UTC 25 Oct	4.5	8.2	0200 UTC 25 Oct	4.1	8.3	0500 UTC 25 Oct	Wilma
44017	2.5	10	0800 UTC 17 Sep	2.3	9.2	1300 UTC 17 Sep	2.5	9.6	1300 UTC 17 Sep	Ophelia
(45 m)	3.7	9.1	0900 UTC 9 Oct	3.6	8.4	0800 UTC 9 Oct	3.7	8.6	0900 UTC 9 Oct	SD22
	5.3	9.1	2300 UTC 12 Oct	4.5	9.2	1000 UTC 13 Oct	4.6	9.3	1000 UTC 13 Oct	SD24
	6.8	9.1	1400 UTC 25 Oct	4.4	8.1	1000 UTC 25 Oct	4.7	9.5	2000 UTC 25 Oct	Wilma
44018	2.6	12.2	1900 UTC 17 Sep	3.0	9.9	1800 UTC 17 Sep	3.5	10.3	1700 UTC 17 Sep	Ophelia
(74 m)	2.8	7.4	2100 UTC 9 Oct	3.1	8.7	1900 UTC 9 Oct	3.3	8.6	1700 UTC 9 Oct	SD22
	5.1	7.3	0000 UTC 13 Oct	4.8	9.3	1000 UTC 13 Oct	4.9	9.3	1000 UTC 13 Oct	SD24
	6.9	10.8	1500 UTC 25 Oct	5.9	9.4	2100 UTC 25 Oct	6.3	9.5	1900 UTC 25 Oct	Wilma
44025	2.3	8.7	1900 UTC 7 Sep	1.6	9.4	1500 UTC 7 Sep	1.6	8.9	1700 UTC 7 Sep	Maria
(36 m)	2.4	11.1	0600 UTC 17 Sep	2.0	8.8	1200 UTC 17 Sep	2.1	9.0	1200 UTC 17 Sep	Ophelia
	4.0	9.1	0500 UTC 9 Oct	3.7	8.3	0400 UTC 9 Oct	3.8	8.2	0400 UTC 9 Oct	SD22
	4.8	12.5	0500 UTC 14 Oct	4.6	9.5	0400 UTC 14 Oct	4.7	9.5	0500 UTC 14 Oct	SD24
	6.0	10.0	1300 UTC 25 Oct	4.7	9.0	1200 UTC 25 Oct	4.4	9.0	1600 UTC 25 Oct	Wilma

APPENDIX B

The Peak Significant Wave Heights (Hs), Simultaneous Spectral Peak Periods (Tp), Times of Occurrence, and Associated Cyclone Names for the Gulf of Mexico–Caribbean Sea

Buoy ID (depth)	Buoy Hs (m)	Buoy Tp (s)	Buoy time and date	NAH Hs (m)	NAH Tp (s)	NAH time and date	WNA Hs (m)	WNA Tp (s)	WNA time and date	Name of TC
42001	3.8	11.4	0900 UTC 11 Jun	2.9	10.1	1800 UTC 11 Jun	2.7	8.4	1000 UTC 11 Jun	Arlene
(3246 m)	3.1	7.7	1300 UTC 5 Jul	4.6	8.4	1500 UTC 5 Jul	2.8	7.8	2300 UTC 5 Jul	Cindy
	2.6	12.1	0600 UTC 10 Jul	3.9	13.4	0600 UTC 10 Jul	2.6	10.2	1200 UTC 10 Jul	Dennis
	2.9	11.4	0000 UTC 19 Jul	3.1	12.1	0000 UTC 19 Jul	3.4	10.0	0400 UTC 19 Jul	Emily
	6.7	13.8	1800 UTC 28 Aug	8.0	9.7	2200 UTC 28 Aug	8.0	16.5	1800 UTC 28 Aug	Katrina
	11.6	12.9	2100 UTC 22 Sep	11.8	13.3	1900 UTC 22 Sep	11.0	13.5	1800 UTC 22 Sep	Rita
	2.7	8.3	1200 UTC 3 Oct	2.9	7.6	1100 UTC 3 Oct	2.9	7.5	1200 UTC 3 Oct	Stan
	5.1	10.0	1200 UTC 24 Oct	4.3	8.4	0800 UTC 24 Oct	4.0	8.6	2300 UTC 24 Oct	Wilma
42002	3.6	12.1	1300 UTC 29 Aug	4.2	15.0	0400 UTC 29 Aug	3.8	17.5	0500 UTC 29 Aug	Katrina
(3200 m)	5.0	12.9	1300 UTC 23 Sep	4.9	14.7	0200 UTC 23 Sep	4.4	14.6	0500 UTC 23 Sep	Rita
	2.6	7.7	0700 UTC 4 Oct	2.8	7.7	0500 UTC 4 Oct	2.7	8.0	0500 UTC 4 Oct	Stan
	4.2	10.0	2000 UTC 24 Oct	3.6	8.1	2200 UTC 24 Oct	3.9	10.6	2100 UTC 24 Oct	Wilma
42003	4.9	9.1	2100 UTC 10 Jun	5.6	10.2	2200 UTC 10 Jun	3.1	8.0	2200 UTC 10 Jun	Arlene
(3233 m)	2.1	7.7	0500 UTC 5 Jul	2.7	6.8	1800 UTC 4 Jul	2.4	6.5	1800 UTC 4 Jul	Cindy
	6.0	13.8	0000 UTC 10 Jul	7.1	13.5	2300 UTC 9 Jul	4.8	9.9	0000 UTC 10 Jul	Dennis
	3.0	12.9	1900 UTC 18 Jul	2.3	12.3	1900 UTC 18 Jul	1.9	6.6	1900 UTC 18 Jul	Emily
	10.6	12.9	0500 UTC 28 Aug	8.7	10.7	0700 UTC 28 Aug	12.8	13.1	0700 UTC 28 Aug	Katrina*
	6	10.0	1500 UTC 24 Oct	5.9	9.2	1300 UTC 24 Oct	5.5	6.4	1200 UTC 24 Oct	Wilma
42019	5.3	11.1	0700 UTC 20 Jul	4.5	11.1	0600 UTC 20 Jul	4.5	10.9	0500 UTC 20 Jul	Emily
(82 m)	4.3	14.3	0800 UTC 29 Aug	3.1	14.2	0600 UTC 29 Aug	3.4	14.6	0700 UTC 29 Aug	Katrina
	5.9	12.5	2000 UTC 23 Sep	3.7	13.2	1700 UTC 23 Sep	4.1	14.1	2100 UTC 23 Sep	Rita
	2.9	9.1	1000 UTC 4 Oct	2.8	8.2	1000 UTC 4 Oct	2.8	8.4	0900 UTC 4 Oct	Stan
	4.3	7.7	1200 UTC 24 Oct	3.0	6.7	1200 UTC 24 Oct	3.2	6.8	1100 UTC 24 Oct	Wilma
42020	6.5	11.1	1000 UTC 20 Jul	5.5	11.8	0500 UTC 20 Jul	6.0	11.1	0900 UTC 20 Jul	Emily
(88 m)	3.9	14.3	1500 UTC 29 Aug	3.5	14.1	0900 UTC 29 Aug	3.7	14.9	1100 UTC 29 Aug	Katrina
	5.3	14.3	0400 UTC 24 Sep	3.7	13.2	2000 UTC 23 Sep	3.9	14.0	2100 UTC 23 Sep	Rita
	2.7	9.1	0900 UTC 4 Oct	2.5	8.3	1100 UTC 4 Oct	2.6	8.4	1100 UTC 4 Oct	Stan
	4.2	8.3	1100 UTC 24 Oct	3.1	7.1	1500 UTC 24 Oct	3.2	5.9	1300 UTC 24 Oct	Wilma
42035	2.6	11.1	1500 UTC 20 Jul	2.8	7.2	0400 UTC 20 Jul	2.8	7.0	0300 UTC 20 Jul	Emily
(14 m)	2.8	14.3	0000 UTC 29 Aug	2.8	7.4	0700 UTC 29 Aug	2.9	7.4	0800 UTC 29 Aug	Katrina
	6.1	9.2	0600 UTC 24 Sep	5.7	7.2	0500 UTC 24 Sep	5.5	6.8	0400 UTC 24 Sep	Rita
	2.2	5.9	0800 UTC 24 Oct	2.3	5.4	1000 UTC 24 Oct	2.4	5.4	1000 UTC 24 Oct	Wilma
	2.1	6.3	1500 UTC 4 Oct	2.2	6.4	0900 UTC 4 Oct	2.2	6.5	0900 UTC 4 Oct	Stan
42036	5.5	12.5	0900 UTC 29 Aug	5.9	9.7	1600 UTC 29 Aug	5.3	11.1	1600 UTC 29 Aug	Katrina
(55 m)	4.1	11.1	0400 UTC 23 Sep	3.6	9.5	1600 UTC 22 Sep	3.6	10.7	0400 UTC 23 Sep	Rita
	2.9	7.1	0400 UTC 5 Oct	2.3	5.8	0400 UTC 5 Oct	2.3	5.7	0400 UTC 5 Oct	Stan
	4.7	8.3	1700 UTC 24 Oct	4.6	7.7	1900 UTC 24 Oct	3.7	6.9	1600 UTC 24 Oct	Wilma
42039	6.4	11.4	0900 UTC 11 Jun	9.5	11.3	0900 UTC 11 Jun	5.2	9.1	0800 UTC 11 Jun	Arlene
(291 m)	2.4	7.1	1800 UTC 6 Jul	2.4	7.0	1700 UTC 6 Jul	2.4	6.9	1600 UTC 6 Jul	Cindy
	8.1	11.4	1400 UTC 29 Aug	7.4	10.26	1600 UTC 29 Aug	7.7	12.8	1100 UTC 29 Aug	Katrina
	5.3	11.4	2100 UTC 22 Sep	4.8	11.20	1700 UTC 22 Sep	5.0	12.0	2300 UTC 22 Sep	Rita
	3	8.3	0800 UTC 5 Oct	2.6	6.75	0800 UTC 5 Oct	2.6	6.6	0600 UTC 5 Oct	Stan
	4.1	7.1	1200 UTC 24 Oct	4.3	7.49	1400 UTC 24 Oct	4.0	7.1	1400 UTC 24 Oct	Wilma
42040	5.4	12.5	1200 UTC 11 Jun	5.8	11.11	1300 UTC 11 Jun	3.9	9.1	1400 UTC 11 Jun	Arlene
(444 m)	16.9	14.3	1100 UTC 29 Aug	12.2	13.36	1000 UTC 29 Aug	15.5	13.9	1200 UTC 29 Aug	Katrina
	7.0	8.9	0200 UTC 23 Sep	5.6	12.71	1900 UTC 22 Sep	6.5	12.0	0900 UTC 23 Sep	Rita
	3.3	8.3	1200 UTC 5 Oct	2.5	7.02	1100 UTC 5 Oct	2.4	7.0	1100 UTC 5 Oct	Tammy
	4.3	8.3	1300 UTC 24 Oct	3.7	7.03	1400 UTC 24 Oct	3.6	6.3	1000 UTC 24 Oct	Wilma
42055	3.1	12.9	0900 UTC 29 Aug	2.5	15.90	0400 UTC 29 Aug	2.2	12.3	0700 UTC 29 Aug	Katrina
(3381 m)	3.9	14.8	1600 UTC 22 Sep	3.7	14.10	0000 UTC 23 Sep	3.3	12.4	2100 UTC 22 Sep	Rita
	3.7	10.0	0600 UTC 25 Oct	3.4	9.26	1200 UTC 25 Oct	3.5	9.3	1200 UTC 25 Oct	Wilma
	3.5	9.1	0900 UTC 4 Oct	4.3	8.83	0900 UTC 4 Oct	3.7	8.2	0400 UTC 4 Oct	Stan
42056	11	12.1	0800 UTC 21 Oct	10.5	11.42	0000 UTC 21 Oct	14.4	13.0	0500 UTC 21 Oct	Wilma
(4446 m)	3.5	7.7	0600 UTC 30 Oct	3.2	7.02	1600 UTC 30 Oct	3.3	7.2	1600 UTC 30 Oct	Beta

APPENDIX B (*Continued*)

Buoy ID (depth)	Buoy Hs (m)	Buoy Tp (s)	Buoy time and date	NAH Hs (m)	NAH Tp (s)	NAH time and date	WNA Hs (m)	WNA Tp (s)	WNA time and date	Name of TC
42057	6.1	8.3	1400 UTC 19 Oct	3.4	7.4	1100 UTC 19 Oct	2.9	7.4	1500 UTC 19 Oct	Wilma
(293 m)	1.7	6.3	1700 UTC 29 Oct	2.5	6.5	2100 UTC 29 Oct	2.4	6.3	1800 UTC 29 Oct	Beta

APPENDIX C

The 5-Day Error Statistics for NAH and WNA Modeled Significant Wave Heights (Hs, m) for All Available Tropical Cyclones at All Available Buoys

Case No.	TC name	Buoy ID	NAH-Hs RMSE	BIAS	COR	SI (%)	*a*	*b*	WNA-Hs RMSE	BIAS	COR	SI (%)	*a*	*b*
1	Maria	41001	0.30	−0.01	0.88	11.3	0.99	0.05	0.28	−0.08	0.91	10.6	1.02	0.04
2	Ophelia	41001	0.66	0.54	0.97	23.4	0.73	0.22	0.36	0.23	0.97	12.7	0.89	0.09
3	Wilma	41001	0.58	0.37	0.93	21.4	0.81	0.15	0.61	0.38	0.91	22.7	0.78	0.23
4	Nate	41002	0.32	−0.01	0.81	11.7	0.93	0.19	0.30	−0.12	0.87	11.1	1.03	0.03
5	Ophelia	41002	0.84	−0.50	0.82	18.0	0.93	−0.18	0.55	−0.06	0.87	11.9	0.89	0.44
6	Tammy	41002	0.31	−0.10	0.94	12.2	1.25	−0.54	0.38	−0.18	0.95	14.8	1.37	−0.78
7	Wilma	41002	0.29	−0.17	0.97	15.8	0.89	0.38	0.30	−0.24	0.98	16.8	0.96	0.31
8	Katrina	41010	0.25	0.08	0.93	16.9	0.92	0.19	0.28	0.14	0.93	19.3	0.99	0.16
9	Ophelia	41010	0.77	0.55	0.72	22.1	0.79	0.19	0.85	0.67	0.66	24.6	0.29	1.75
10	Rita	41010	0.41	0.29	0.91	20.8	0.73	0.24	0.39	0.25	0.89	19.9	0.78	0.18
11	Tammy	41010	0.38	−0.12	0.91	12.3	1.25	−0.65	0.32	−0.12	0.92	10.3	1.15	−0.36
12	Wilma	41010	0.66	0.04	0.93	33.2	0.97	0.09	0.37	0.03	0.98	18.7	1.01	0.00
13	Philippe	41040	0.21	0.07	0.90	9.7	0.70	0.57	0.25	0.11	0.86	11.5	0.67	5.91
14	Wilma	41040	0.36	−0.07	0.87	15.9	0.70	0.75	0.34	−0.10	0.89	15.2	0.75	0.66
15	Philippe	41041	0.44	−0.26	0.36	21.2	0.75	0.73	0.38	−0.24	0.38	19.9	0.77	0.67
16	Wilma	41041	0.38	−0.23	0.85	17.0	0.80	0.68	0.39	−0.23	0.83	16.8	0.77	0.77
17	Maria	44004	0.20	0.01	0.90	9.2	1.07	−0.15	0.22	0.01	0.88	10.2	1.06	−0.14
18	Ophelia	44004	0.37	−0.01	0.97	20.0	0.78	0.42	0.37	−0.18	0.97	19.9	0.88	0.42
19	Wilma	44004	1.05	0.65	0.91	29.6	0.64	0.65	0.98	0.58	0.91	27.5	0.67	0.59
20	Arlene	42001	0.25	0.01	0.96	20.5	0.85	0.19	0.27	0.04	0.97	22.0	0.75	0.27
21	Cindy	42001	0.44	0.22	0.97	39.2	1.26	−0.08	0.25	0.09	0.97	22.1	0.91	0.19
22	Dennis	42001	0.69	0.30	0.90	60.0	1.60	−0.39	0.25	−0.01	0.92	21.7	0.89	0.12
23	Emily	42001	0.34	0.21	0.94	21.9	1.23	−0.15	0.37	0.18	0.93	23.4	1.29	−0.27
24	Katrina	42001	0.61	−0.11	0.96	20.8	1.02	0.04	0.53	−0.21	0.98	18.0	1.09	−0.05
25	Rita	42001	0.76	−0.16	0.96	18.1	0.97	−0.01	0.78	−0.11	0.96	18.6	0.85	0.51
26	Stan	42001	0.35	−0.25	0.94	18.8	1.08	0.10	0.39	−0.30	0.94	20.7	1.07	0.16
27	Wilma	42001	0.54	−0.23	0.92	18.3	0.66	1.22	0.54	−0.21	0.93	18.4	0.60	1.37
28	Katrina	42002	0.52	−0.10	0.89	37.8	1.05	0.03	0.58	−0.03	0.82	42.0	0.89	0.18
29	Rita	42002	0.68	0.19	0.86	27.9	0.87	0.14	0.41	0.20	0.96	16.9	0.90	0.04
30	Stan	42002	0.33	−0.01	0.94	19.4	1.32	−0.53	0.30	0.02	0.93	17.4	1.24	−0.42
31	Wilma	42002	0.30	−0.18	0.96	14.6	0.80	0.60	0.32	−0.26	0.97	15.5	0.80	0.47
32	Arlene	42003	0.49	0.25	0.97	35.7	1.29	−0.15	0.38	−0.05	0.92	27.1	0.77	0.27
33	Cindy	42003	0.33	0.07	0.90	29.5	1.33	−0.30	0.28	0.06	0.91	24.8	1.24	−0.21
34	Dennis	42003	0.93	0.27	0.92	50.1	1.35	−0.37	0.39	−0.13	0.96	20.9	0.91	0.04
35	Emily	42003	0.34	0.21	0.94	21.9	1.23	−0.15	0.37	0.18	0.93	23.4	1.29	−0.27
36	Katrina	42003	1.86	1.71	0.91	25.2	0.97	−1.48	1.40	0.35	0.89	19.0	1.44	−3.62
37	Wilma	42003	0.87	0.31	0.70	22.9	0.63	1.09	0.78	0.08	0.73	20.3	0.64	1.30
38	Arlene	42039	0.77	0.23	0.97	47.5	1.38	−0.39	0.36	−0.13	0.98	22.2	0.87	0.08
39	Cindy	42039	0.17	−0.04	0.97	14.7	0.99	−0.03	0.15	−0.01	0.98	12.6	1.02	−0.04
40	Katrina	42039	0.57	0.24	0.98	13.5	0.87	0.31	0.45	−0.01	0.98	10.6	0.95	0.22
41	Rita	42039	0.50	−0.06	0.92	16.1	0.96	0.17	0.27	0.01	0.98	8.7	1.05	−0.17
42	Stan	42039	0.20	0.13	0.98	10.9	0.91	0.04	0.19	0.11	0.97	10.5	0.92	0.04
43	Wilma	42039	0.68	0.32	0.66	26.5	0.97	−0.23	0.69	0.19	0.59	27.0	0.89	0.08
44	Arlene	42040	0.48	−0.15	0.95	32.3	0.99	−0.13	0.61	−0.33	0.96	40.6	0.67	0.13

APPENDIX C (*Continued*)

Case No.	TC name	Buoy ID	NAH-Hs RMSE	NAH-Hs BIAS	NAH-Hs COR	NAH-Hs SI (%)	NAH-Hs *a*	NAH-Hs *b*	WNA-Hs RMSE	WNA-Hs BIAS	WNA-Hs COR	WNA-Hs SI (%)	WNA-Hs *a*	WNA-Hs *b*
45	Katrina	42040	1.12	−0.55	0.98	25.0	0.82	0.27	0.63	−0.03	0.99	14.1	1.00	−0.04
46	Rita	42040	0.67	0.31	0.96	18.0	0.83	0.34	0.34	0.08	0.99	9.2	1.00	−0.08
47	Wilma	42040	0.51	−0.19	0.86	26.1	0.64	0.90	0.72	–0.38	0.74	36.8	0.65	1.08
48	Katrina	42055	0.32	0.14	0.94	23.8	0.78	0.15	0.32	0.17	0.95	24.1	0.76	0.15
49	Rita	42055	0.53	0.36	0.92	24.7	0.88	−0.10	0.50	0.34	0.94	23.1	0.76	0.17
50	Stan	42055	0.39	−0.15	0.99	24.3	1.27	−0.28	0.30	−0.07	0.98	18.4	1.14	−0.15
51	Wilma	42055	0.22	−0.09	0.97	10.4	0.82	0.48	0.19	−0.06	0.97	8.7	0.91	0.26
52	Wilma	42056	1.49	−0.58	0.83	24.4	0.81	0.56	1.30	0.86	0.96	21.3	1.21	−0.44
53	Beta	42056	0.23	−0.09	0.96	10.7	0.87	0.18	0.22	−0.04	0.95	10.1	0.92	0.13
54	Wilma	42057	1.78	1.22	0.46	49.4	0.24	1.53	2.08	1.56	0.34	57.6	0.11	1.66
55	Beta	42057	0.46	−0.32	0.54	33.2	0.76	0.66	0.47	−0.34	0.53	34.4	0.77	0.65

APPENDIX D

The 5-Day Error Statistics for NAH and WNA Modeled Wind Speeds at 10-m Height (U_{10}, m s^{-1}) for All Available Tropical Cyclones at All Available Buoys

Case No.	TC name	Buoy ID	NAH-Hs RMSE	NAH-Hs BIAS	NAH-Hs COR	NAH-Hs SI (%)	NAH-Hs *a*	NAH-Hs *b*	WNA-Hs RMSE	WNA-Hs BIAS	WNA-Hs COR	WNA-Hs SI (%)	WNA-Hs *a*	WNA-Hs *b*
1	Maria	41001	0.90	−0.26	0.95	10.9	0.95	0.66	0.87	−0.42	0.96	10.6	1.00	0.46
2	Ophelia	41001	1.17	−0.41	0.92	13.4	0.85	1.68	1.39	−0.89	0.95	16.0	1.10	−0.02
3	Wilma	41001	1.54	−0.23	0.93	17.5	0.90	1.09	1.24	−0.27	0.96	14.2	0.92	0.95
4	Nate	41002	1.23	0.64	0.73	11.9	0.50	4.56	0.94	0.37	0.84	9.0	0.62	3.77
5	Ophelia	41002	3.53	−0.30	0.80	22.0	1.38	−6.43	2.84	0.91	0.83	17.7	1.21	−2.46
6	Tammy	41002	0.98	0.22	0.91	9.5	0.73	2.59	0.85	0.03	0.93	8.3	0.77	2.34
7	Wilma	41002	1.46	−0.20	0.89	20.7	0.74	2.04	1.47	−0.33	0.89	20.8	0.78	1.86
8	Katrina	41010	1.22	0.48	0.89	19.0	0.93	0.95	1.08	0.59	0.94	16.8	1.00	0.56
9	Ophelia	41010	3.30	−1.47	0.78	28.5	1.22	−1.18	2.25	0.66	0.74	19.5	0.76	2.09
10	Rita	41010	0.88	0.39	0.92	11.9	0.88	0.46	0.85	0.33	0.92	11.6	0.91	0.34
11	Tammy	41010	1.46	−0.23	0.77	13.6	0.88	1.56	1.13	−0.05	0.82	10.6	0.70	3.29
12	Wilma	41010	2.37	0.64	0.95	35.1	1.14	−0.32	2.26	0.64	0.96	33.6	1.16	−0.46
13	Philippe	41040	2.01	0.11	0.45	25.6	0.34	5.10	1.80	0.23	0.58	22.9	0.45	4.06
14	Wilma	41040	0.90	0.11	0.77	13.6	0.79	1.29	0.90	0.10	0.77	13.6	0.79	1.28
15	Philippe	41041	1.51	−0.62	0.71	24.2	0.74	2.23	1.46	−0.61	0.72	23.4	0.74	2.26
16	Wilma	41041	1.04	−0.03	0.80	15.4	0.76	1.66	1.04	−0.03	0.8	15.4	0.76	1.68
17	Maria	44004	0.64	−0.10	0.98	9.3	0.96	0.40	0.67	−0.22	0.98	9.8	0.97	0.44
18	Ophelia	44004	2.13	−1.12	0.90	36.9	0.77	2.42	2.24	−1.25	0.89	38.8	0.84	2.20
19	Wilma	44004	2.52	0.36	0.83	21.2	0.81	1.97	2.65	0.04	0.8	22.2	0.76	2.81
20	Arlene	42001	1.18	0.14	0.79	22.5	0.66	1.89	0.85	−0.02	0.9	16.0	0.74	1.34
21	Cindy	42001	2.34	−0.32	0.90	36.8	1.10	−0.93	1.49	−0.85	0.96	23.4	0.85	0.09
22	Dennis	42001	1.39	0.05	0.81	23.2	1.01	−0.03	0.98	−0.42	0.89	16.4	0.75	1.05
23	Emily	42001	1.30	−0.25	0.78	15.6	0.73	2.00	1.24	−0.20	0.80	15.0	0.78	1.67
24	Katrina	42001	2.74	−0.18	0.92	26.2	1.08	−0.70	2.89	−0.88	0.96	27.7	1.26	−1.88
25	Rita	42001	4.83	−1.31	0.85	32.4	0.73	2.74	5.32	−0.90	0.80	35.7	0.64	4.41
26	Stan	42001	1.23	0.62	0.77	12.1	0.60	3.41	1.15	0.48	0.78	11.3	0.59	3.68
27	Wilma	42001	1.01	−0.08	0.96	10.3	1.01	0.47	1.01	−0.08	0.96	10.3	0.84	1.62
28	Katrina	42002	1.41	0.14	0.82	23.8	0.95	0.14	1.29	0.54	0.83	21.7	0.69	1.28
29	Rita	42002	1.76	0.48	0.76	19.5	0.63	2.81	1.25	0.56	0.91	13.9	0.73	1.92
30	Stan	42002	1.30	0.84	0.81	14.7	0.80	0.97	1.28	0.90	0.83	14.5	0.76	1.27
31	Wilma	42002	1.13	−0.38	0.91	14.8	0.74	2.37	1.16	−0.58	0.92	15.1	0.81	2.07
32	Arlene	42003	3.69	1.57	0.59	57.4	0.87	2.40	2.24	0.28	0.63	34.9	0.52	3.35
33	Cindy	42003	1.34	0.19	0.91	21.4	0.99	0.25	1.10	0.06	0.93	17.6	0.95	0.39
34	Dennis	42003	3.45	1.29	0.92	43.2	1.37	−1.68	1.55	0.56	0.97	19.3	1.10	−0.26
35	Emily	42003	1.04	−0.45	0.79	14.1	0.85	0.68	1.04	−0.45	0.79	14.1	0.85	0.68
36	Katrina	42003	3.15	1.98	0.88	15.6	1.02	−2.47	4.09	−1.80	0.92	20.3	1.55	−9.31

APPENDIX D (*Continued*)

Case No.	TC name	Buoy ID	NAH-Hs						WNA-Hs					
			RMSE	BIAS	COR	SI (%)	*a*	*b*	RMSE	BIAS	COR	SI (%)	*a*	*b*
37	Wilma	42003	1.58	−0.81	0.93	15.0	0.94	1.47	1.58	−0.86	0.94	15.0	0.99	1.00
38	Arlene	42039	2.95	1.00	0.91	40.9	1.24	−0.76	1.29	0.28	0.96	17.8	0.97	0.50
39	Cindy	42039	1.04	0.39	0.94	20.0	0.84	1.21	1.07	0.41	0.93	20.4	0.84	1.26
40	Katrina	42039	2.18	−0.90	0.95	19.3	1.28	−2.24	1.21	−0.33	0.97	10.7	1.13	−1.14
41	Rita	42039	2.28	−1.16	0.76	21.7	1.07	0.42	1.49	−0.54	0.84	14.2	1.00	0.49
42	Stan	42039	0.87	−0.32	0.90	9.3	0.92	1.11	0.95	−0.40	0.90	9.9	0.94	0.95
43	Wilma	42039	1.78	−1.27	0.97	22.7	1.04	0.91	1.20	−0.86	0.98	15.3	0.93	1.43
44	Arlene	42040	2.41	0.91	0.93	42.1	1.22	−0.37	1.40	0.63	0.96	24.5	1.01	0.56
45	Katrina	42040	2.62	0.97	0.96	22.8	1.19	−1.20	3.71	1.89	0.97	32.2	1.40	−2.74
46	Rita	42040	1.42	−0.46	0.91	12.6	0.94	1.10	1.52	−1.00	0.97	13.5	1.17	−0.92
47	Wilma	42040	1.42	−0.85	0.96	17.6	1.03	0.58	1.17	−0.68	0.97	14.5	0.97	0.92
48	Katrina	42055	1.24	−0.03	0.77	23.6	0.76	1.31	1.15	0.09	0.78	22.1	0.66	1.71
49	Rita	42055	1.13	0.29	0.88	16.2	1.00	−0.30	0.97	0.55	0.92	13.8	0.86	0.40
50	Stan	42055	1.82	0.28	0.88	23.4	0.92	0.33	1.60	0.22	0.90	21.0	0.93	0.31
51	Wilma	42055	1.18	0.40	0.88	13.9	0.66	2.53	1.10	0.29	0.89	13.0	0.68	2.43
52	Wilma	42056	4.20	−2.47	0.79	21.5	0.80	1.50	3.00	1.94	0.95	15.3	1.22	−2.27
53	Beta	42056	2.18	−1.72	0.92	21.0	0.92	−0.91	2.11	−1.63	0.92	20.4	0.95	−1.06
54	Wilma	42057	4.81	2.16	0.51	36.8	0.55	3.67	5.03	3.39	0.54	38.4	0.45	3.85
55	Beta	42057	1.83	−0.83	0.58	26.6	0.41	4.90	2.55	−1.45	0.44	37.0	0.44	5.33

REFERENCES

Alves, J. H. G. M., H. L. Tolman, and Y. Y. Chao, 2004: Hurricane-generated wind-wave research at NOAA/NCEP. Preprints, *Eighth Int. Workshop on Wave Hindcasting and Forecasting,* Turtle Bay, HI, U.S. Army Engineer Coastal and Hydraulics Lab., Environment Canada, and WMO/IOC/JCOMM, G3, 13 pp.

Bender, M. A., I. Ginis, R. Tuleya, B. Thomas, and T. Marchok, 2007: The operational GFDL coupled hurricane-ocean prediction system and a summary of its performance. *Mon. Wea. Rev.,* **135,** 3965–3989.

Bidlot, J. R., D. J. Holmes, P. A. Whittman, R. Lalbeharry, and H. S. Chen, 2002: Intercomparison of the performance of operational ocean wave forecasting systems with buoy data. *Wea. Forecasting,* **17,** 287–310.

Caplan, P., J. Derber, W. Gemmill, S. Y. Hong, H. L. Pan, and D. Parish, 1997: Changes to the 1995 NCEP operational medium-range forecast model analysis–forecast system. *Wea. Forecasting,* **12,** 581–594.

Chao, Y. Y., and H. Tolman, 2000: Numerical experiments on predicting hurricane generated wind waves. Preprints, *Sixth Int. Workshop on Wave Hindcasting and Forecasting,* Monterey, CA, U.S. Army Engineer Research and Development Center, 167–179.

——, and ——, 2001: Specification of hurricane wind fields for ocean wave prediction. *Proc. Fourth Int. Symp. on Waves: Ocean Wave Measurement and Analysis,* Vol. 1, San Francisco, CA, Office of Naval Research, 671–679.

——, L. D. Burroughs, and H. L. Tolman, 2003a: The North Atlantic Hurricane wind wave forecasting system (NAH). Tech. Procedure Bull. 478, National Weather Service, 6 pp. [Available online at http://polar.ncep.noaa.gov/mmab/tpbs/operational.tpbs/tpb478/tpb478.htm.]

——, ——, and ——, 2003b: Wave forecasting for the western North Atlantic and adjacent waters. Tech. Procedure Bull. 495, National Weather Service, 12 pp. [Available online at http://polar.ncep.noaa.gov/mmab/tpbs/operational.tpbs/tpb495/tpb495.htm.]

——, J. H. G. M. Alves, and H. L. Tolman, 2005: An operational system for predicting hurricane-generated wind waves in the North Atlantic Ocean. *Wea. Forecasting,* **20,** 652–671.

Chawla, A., D. Cao, V. Gerald, and H. L. Tolman, 2007: Operational implementation of a multi-grid wave forecasting system. Preprints, *10th Int. Workshop on Wave Hindcasting and Forecasting and Coastal Hazard Symposium,* Turtle Bay, HI, U.S. Army Engineer Coastal and Hydraulics Lab., Environment Canada, and WMO/IOC/JCOMM, B3, 12 pp.

NCDC, cited 2006: Climate of 2005 Atlantic Hurricane Season. National Climatic Data Center. [Available online at http://www.ncdc.noaa.gov/oa/climate/research/2005/hurricanes05.html.]

Tolman, H. L., 2002a: The 2002 release of WAVEWATCH III. Preprints, *Seventh Int. Workshop on Wave Hindcasting and Forecasting,* Banff, AB, Canada, Environment Canada, 188–197.

——, 2002b: User manual and system documentation of WAVE WATCH III version 2.22. OMB Tech. Note 222, NWS/Ocean Modeling Branch, 133 pp.

——, 2008: A mosaic approach to wind wave modeling. *Ocean Modell.,* **25,** 35–47.

——, B. Balasubramaniyan, L. D. Burroughs, D. V. Chahlikov, Y. Y. Chao, H. S. Chen, and V. M. Gerald, 2002: Development and implementation of wind-generated ocean surface wave models at NCEP. *Wea. Forecasting,* **17,** 311–333.

——, J. H. G. M. Alves, and Y. Y. Chao, 2005: Operational forecasting of wind-generated waves by Hurricane Isabel at NCEP. *Wea. Forecasting,* **20,** 544–557.

Wright, C. W., and Coauthors, 2001: Hurricane directional wave spectrum spatial variation in the open ocean. *J. Phys. Oceanogr.,* **31,** 2472–2488.